AD-A053 620 SRI INTERNATIONAL MENLO PARK CA F/G 4/2
EVALUATION OF THE FIB METHODOLOGY FOR APPLICATION TO CLOUD MOTI--ETC(U)
JUL 77 W VIEZEE, D E WOLF, R M ENDLICH N00228-76-C-3182
UNCLASSIFIED SRI-TR-77-08 NL

1 OF 1
ADA
053620

END
DATE
FILMED
6-78
DDC

10

Technical Report TR-77-08 (SRI)

EVALUATION OF THE FIB METHODOLOGY FOR APPLICATION TO CLOUD MOTION WIND DATA

Prepared by:

WILLIAM VIEZEE
DANIEL E. WOLF
ROY M. ENDLICH
SRI International
333 Ravenswood Avenue
Menlo Park, California 94025

23 July 1977

Final Report for Period 23 June 1976-23 June 1977

Approved for public release; distribution unlimited

Prepared for:

NAVAL AIR SYSTEMS COMMAND
Department of the Navy
Washington, D.C. 20361

NAVAL ENVIRONMENTAL PREDICTION RESEARCH FACILITY
Monterey, California 93940

STANFORD RESEARCH INSTITUTE
Menlo Park, California 94025 · U.S.A.

UNCLASSIFIED

SECURITY CLASSIFICATION OF THIS PAGE (When Data Entered)

REPORT DOCUMENTATION PAGE

READ INSTRUCTIONS BEFORE COMPLETING FORM

1. REPORT NUMBER: Technical Report: SRI-TR-77-08 (SRI)

2. GOVT ACCESSION NO.

3. RECIPIENT'S CATALOG NUMBER

4. TITLE (and Subtitle): EVALUATION OF THE FIB METHODOLOGY FOR APPLICATION TO CLOUD MOTION WIND DATA

5. TYPE OF REPORT & PERIOD COVERED: Final Report Covering Period 23 June 76 - 23 June 1977

6. PERFORMING ORG. REPORT NUMBER: SRI Project ERU 5551

7. AUTHOR(s): William Viezee, Daniel E. Wolf, Roy M. Endlich

8. CONTRACT OR GRANT NUMBER(s): N00228-76-C-3182

9. PERFORMING ORGANIZATION NAME AND ADDRESS: SRI International, 333 Ravenswood Ave., Menlo Park, California 94025

10. PROGRAM ELEMENT, PROJECT, TASK AREA & WORK UNIT NUMBERS: Air Task A370370G/076B/7F52-551-000 NEPRF WV 086:2-12

11. CONTROLLING OFFICE NAME AND ADDRESS: Naval Air Systems Command, Department of the Navy, Washington, D.C. 20361

12. REPORT DATE: July 1977

13. NO. OF PAGES: 98

14. MONITORING AGENCY NAME & ADDRESS (if diff. from Controlling Office): Naval Environmental Prediction Research Facility, Monterey, California 93940

15. SECURITY CLASS. (of this report): Unclassified

15a. DECLASSIFICATION/DOWNGRADING SCHEDULE

16. DISTRIBUTION STATEMENT (of this report)

Approved for public release; distribution unlimited

16 F52551

17. DISTRIBUTION STATEMENT (of the abstract entered in Block 20, if different from report)

18. SUPPLEMENTARY NOTES

19. KEY WORDS (Continue on reverse side if necessary and identify by block number)

Satellite meteorology
Cloud motion winds
Objective analysis technique

20. ABSTRACT (Continue on reverse side if necessary and identify by block number)

A comprehensive technique for the objective analysis of scalar and vector fields was developed by Holl et al. (1971) under Navy contracts. The technique is called the Fields by Information Blending (FIB) technique. It assimilates or blends available independent observations into a corresponding background field through a least-square-fit procedure. The characteristics of FIB permit, by control of a set of weighting factors, the conservation of background analysis patterns related to gradients and curvature. Furthermore, by manipulation of build-in constraints on the degree of change allowed in the resultant analysis,

over

DD FORM 1 JAN 73 1473

EDITION OF 1 NOV 65 IS OBSOLETE

UNCLASSIFIED

SECURITY CLASSIFICATION OF THIS PAGE (When Data Entered)

AD A040281

19. KEY WORDS (Continued)

20 ABSTRACT (Continued)
features in the independent set of observations can be either suppressed or emphasized in the blending cycle.

This report describes the results of a research study to evaluate the application of the FIB technique to the blending of satellite-derived cloud motion wind data and their finite-difference derivatives (e.g., vorticity and divergence) with conventional wind analyses. The FIB program was supplied to SRI by NEPRF as part of a set of computer programs that, after adaption to SRI's CDC-6400 computer, allowed for the processing, analyses, and subsequent blending of selected trial data sets.

Conclusions are based on the results obtained by executing FIB on the data of two case studies, one of the passage of Hurricane Carmen through the Gulf of Mexico (1-7 September 1974) and the other of the migration of an extratropical cyclone in the eastern North Pacific Ocean (5-8 February 1976). Both areas are over water and are relatively sparse in conventional data, so meteorological analyses could benefit from the assimilation of cloud motion data.

It is concluded that the FIB program and its associated program segments are operationally suitable for blending cloud motion data with conventional wind analyses. However, quality control of the cloud motion vector data must be exercised. Interaction with the computer program is required to judge whether features in the cloud motion data that appear anomalous with respect to the available conventional analyses should be suppressed or maintained in the blending cycle. Such judgment depends on (1) the accuracy of the technique used to determine cloud motions and their height levels, and, more importantly, on (2) the validity of the assumed relation of cloud motion vectors to the wind field.

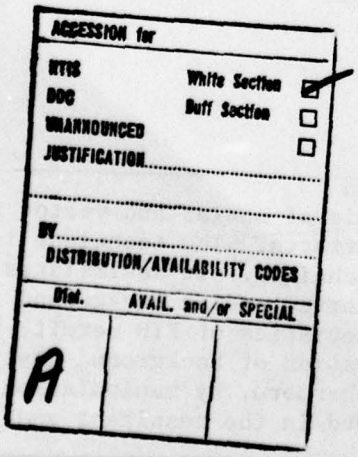

CONTENTS

ILLUSTRATIONS*

*Only the illustrations for the main body of the report are listed

I INTRODUCTION AND OBJECTIVES

An operational, objective-analysis technique called fields by information blending (FIB) was developed by Holl et al. (1971)* for producing sea-surface temperature analyses and by Holl and Mendenhall (1971) for sea-level pressure analyses at Fleet Numerical Weather Central, Monterey, California. The FIB technique includes the capability of exploiting both sea-surface temperature information from satellites in temperature analyses and surface wind observations in pressure analyses. A third version of FIB was formulated for application to wind analyses; it can directly assimilate information in the form of (1) wind values in two components, (2) vorticity in the grid scale, and (3) divergence in the grid scale. An upper-air analysis procedure applying FIB to blend independent wind information with a height-contour field was described by Schiessl (1975).

Under Contract N00228-76-C-3182, SRI International evaluated an operationally oriented computer program organized and developed by NEPRF. This program enables investigation of the objective FIB technique for blending satellite-observed cloud motion data with conventional wind observations. The overall objective of the evaluation study was to assess the validity of the FIB technique and the associated program elements as a means to assimilate cloud motion vector data with other conventional environment analyses. The specific objectives were:

(1) To gain familiarity with the NEPRF computer program, adapt its execution to the SRI CDC-6400 computer, and demonstrate the success of a test execution of it.

(2) To test and evaluate the blending (FIB) technique, using different options in the program, including:

    (a) Direct blending of the radiosonde winds and cloud motion vectors, with differing weighting factors.

---

*References are listed at the end of the report.

(b) Blending using the vorticity and divergence from the cloud motion analyses, with differing weighting factors.

(3) To apply the blending technique to two separate case studies involving both high- and low-level clouds, and to assess the meteorological significance of the resulting analyses.

This final report describes the results of the research study. Background information on the interest in applying FIB to cloud motion winds is provided in Section II. An overview of the FIB methodology is given in Section III. A discussion of the research study, in Section IV, is followed by conclusions and recommendations, in Section V. Applications of the FIB technique to the cloud motion data and the conventional observations used in the two test case studies are described in detail in the Appendices.

II BACKGROUND

Geosynchronous Meteorological Satellites provide observations of the earth's cloud cover in the visible and infrared portion of the electromagnetic spectrum, with spatial resolution ranging from 0.5 to 2 nmi over time intervals as long as 30 minutes or as short as 7.5 minutes (Gentry et al, 1976). Successive positions of tracer clouds are measured in a sequence of satellite images. The positions are transformed into earth-based coordinates of latitude and longitude, and from the successive changes of the coordinates cloud motion vectors are calculated.

Over the past decade, considerable effort has been expended to relate cloud motion vectors to the wind fields in which the clouds are embedded. A recent study by Suchman and Martin (1976) concluded that cloud motions represent the flow at cumulus and cirrus levels to within the 3.0 ms^{-1} accuracy of currently available ground truth data (e.g., surface ship winds and aircraft winds). Bauer (1976), on the basis of a comparison between cloud motion winds and coinciding radiosonde winds over North America, gave mean absolute differences between a cloud wind and surrounding radiosonde winds of 4.4 ms^{-1} for the u (zonal) component and 4.6 ms^{-1} for the v (meridional) component. An intracomparison of radiosonde winds for the same periods gave mean absolute differences between a radiosonde wind and surrounding reports of 4.2 ms^{-1} for the u component and 5.1 ms^{-1} for the v component. These and associated results suggest that a cloud wind and a radiosonde wind have similar capability to represent atmospheric motions. Smith and Hasler (1976) compared low-level, ATS-3 satellite cloud motion wind estimates with values of wind direction and speed interpolated from analyses based on research aircraft observations of a synoptic tropical wave. Regional vector-magnitude deviations were found to differ to the extent of suggesting that environmental factors peculiar to the regions influenced the movement of the cloud targets. If this

were always true, then evaluation of satellite estimates used to describe the low-level flow in a synoptic tropical wave should be determined on a regional basis.

In general, it is agreed that, over the vast oceanic regions of the world, cloud motions derived from satellites of the GOES and SMS type provide a viable method of obtaining information on the atmospheric motion field. Questions must be posed: What is the information content of cloud motions, and what is the best way to assimilate cloud motion data with other, conventional environment analyses or observations?

The Information Processing and Display Department of the NEPRF has organized a computer program with associated elements, to enable investigation of objective techniques for blending cloud motion data with conventional wind observations. SRI executed this program on a selected number of cases, to evaluate (1) various methods of blending the different types of data and (2) the reality of the resulting wind analyses.

III OVERVIEW OF FIB METHODOLOGY

A. General

The version of the fields by information blending (FIB) technique applied in this study was best documented by Maxwell (1976). His report described the salient features of FIB, which include its ability to conserve gradient and curvature properties of the background and to enable reevaluation or rejection of reports that would cause excessively large changes in the analysis. Since the objective of the study reported here was to apply and evaluate FIB on the basis of case studies rather than to further develop or modify the technique itself, only an overview is presented in this section. For detailed discussions, see Maxwell (1976), Schiessl (1975), Holl et al. (1971), and Holl and Mendenhall (1971).

B. The Methodology

FIB blends independent pieces of information with a corresponding background field through a least-square-fit procedure. The fit is generally performed among the following four information sets, using grid arrays of data:

(1) New, independent data.

(2) The most recent past analysis or current forecast (background field).

(3) Gradients of the background field at each grid point, in four directions.

(4) The Laplacian properties (curvature) of the background field at each grid point.

In this study, the "new data" consisted of cloud motion winds and vorticity and divergence derived therefrom, while the "background field" consisted of an analysis based on conventional radiosonde data.

The FIB analysis is obtained from a numerical solution to the so-called blending equation, which is derived by minimizing the following error functional expression:

$$
\begin{aligned}
E = \sum_{i,j} & A_{i,j} \left(p^*_{i,j} - p_{i,j}\right)^2 \\
& + B_{i,j} \left(p^*_{i,j+1} - p^*_{i,j} - \mu_{i,j}\right)^2 \\
& + C_{i,j} \left(p^*_{i+1,j} - p^*_{i,j} - \nu_{i,j}\right)^2 \\
& + E_{i,j} \left(p^*_{i-1,j+1} - p^*_{i,j} - f_{i,j}\right)^2 \\
& + F_{i,j} \left(p^*_{i+1,j+1} - p^*_{i,j} - g_{i,j}\right)^2 \\
& + D_{i,j} \left(p^*_{i+1,j} + p^*_{i-1,j} + p^*_{i,j+1} + p^*_{i,j-1} \right. \\
& \qquad \left. - 4p^*_{i,j} - L_{i,j}\right)^2
\end{aligned}
\tag{1}
$$

where

$p \equiv$ the scalar quantity of the background field at i,j.

$p^* \equiv$ the scalar quantity to be analyzed at i,j.

$\mu_{i,j} = p_{i,j+1} - p_{i,j} \equiv$ the first gradient of the background field in the j direction.

$\nu_{i,j} = p_{i+1,j} - p_{i,j} \equiv$ the first gradient of the background field in the i direction.

$f_{i,j} = p_{i-1,j+1} - p_{i,j} \equiv$ the first cross gradient of the background field for the left diagonal.

$g_{i,j} = p_{i+1,j+1} - p_{i,j} \equiv$ the first cross gradient of the background field for the right diagonal.

$L_{i,j} = p_{i+1,j} + p_{i-1,j} + p_{i,j+1} + p_{i,j-1} - 4p_{i,j} \equiv$ five-point Laplacian of the background field at i,j.

The pattern-conserving character of FIB is contained in the gradient and Laplacian terms, μ, ν, f, g, and L, in combination with their weights B, C, E, F, and D, respectively.

The optimum solution of the error functional, Eq. (1), is the value of p^* that minimizes the sum of the deviations of the new information set from their counterparts in the background analysis; in other words, the optimum solution determines a value of p^* such that $\frac{\delta E}{\delta p^*} = 0$. Thus, by minimizing E with respect to p^*, Eq. (1) reduces to the so-called blending equation which can be solved for p^*. For a detailed discussion of a solution by the method of successive over-relaxation, refer to Maxwell (1976).

The FIB methodology consists of four major steps:

(1) Assemble the available new, independent data at their grid-point locations in the background field. Where a data point has been assembled, its value replaces the scalar background value at the grid point. This data point is represented by $p_{i,j}$ in the first term of Eq. (1); it is assigned a weight $A_{i,j}$ = DATAWT $_{i,j}$. A point that has no new data associated with it remains equal to the background scalar with weight $A_{i,j}$.

(2) Assign values to the weights A through D in Eq. (1) associated with the various background, scalar, gradient, and curvature properties. Assign to new data values for DATAWT.

(3) Solve the minimization problem (blending equation).

(4) Examine the reliability of each new data point by determining the magnitude of the change it has caused in the background field. If the change exceeds a statistically expected deviation, the influence of the data point can be reduced by reducing the weight of the data point.

C. The FIB Program Evaluated by SRI

The computer program that NEPRF supplied to SRI consists of the following elements:

(1) RSNDAF: This program element extracts from a radiosonde data tape the wind observations at any given isobaric height level for all the stations within a selected area.

(2) LUPWND: This element ingests cloud motion vector end points as derived from a Bendix digitizing board and converts these data to earth-located wind vectors. The motion of the satellite over the observational interval is taken into account, and the vectors are corrected for viewing perspective.

(3) ATSWND: This objective element program produces grid-point values of the motion field from the randomly located cloud motion vectors and from the conventional radiosonde observations. It further computes the relative vorticity and divergence from the grid-point values of the motion fields.

(4) FIB: This element blends an objective analysis of radiosonde winds or kinematic quantities derived therefrom with similar information derived from the cloud motions, in accordance with the relative weights assigned to the different data forms.

Figure 1 summarizes the sequence of data flow in the application of the NEPRF version of the FIB program and its associated program elements. Two streams of analyses merge into the actual data-blending cycle of the FIB technique: One stream operates on the cloud motion vector (CMV) data and the other on the radiosonde (RAWIN) data. If a data tape of earth-located CMV is available, program element LUPWND is not executed, and ATSWND can operate directly on the CMV tape. After ATSWND has generated the desired grid-point analyses, a decision must be made as to which observations constitute the independent, new data sample. It is assumed that normally cloud motion winds are the new information that must be assimilated to upgrade a background analysis based on radiosonde data. However, in conventional-data-sparse areas, such as the tropical and subtropical oceans, where an abundance of high-density CMV winds can become available in connection with the occurrence of a tropical storm, it may be desirable to blend the few available radiosonde winds with a background analysis based on the CMV data. Before the numerical solution to the blending equation is initiated, relative weights must be assigned to the scalar and differential properties of the background analysis, and to the independent data. These weights determine the extent to which the resulting (blended) analysis product is forced to match the gradients and curvature properties of the background field, and to conform to the new data.

In this research, the CMV and RAWIN data of two separate studies were used as test cases to assess the significance of (1) the background vs. independent data selection, (2) the assignment of weighting factors, and (3) the meteorological validity of the blended end product. The results of the research are described in the following sections.

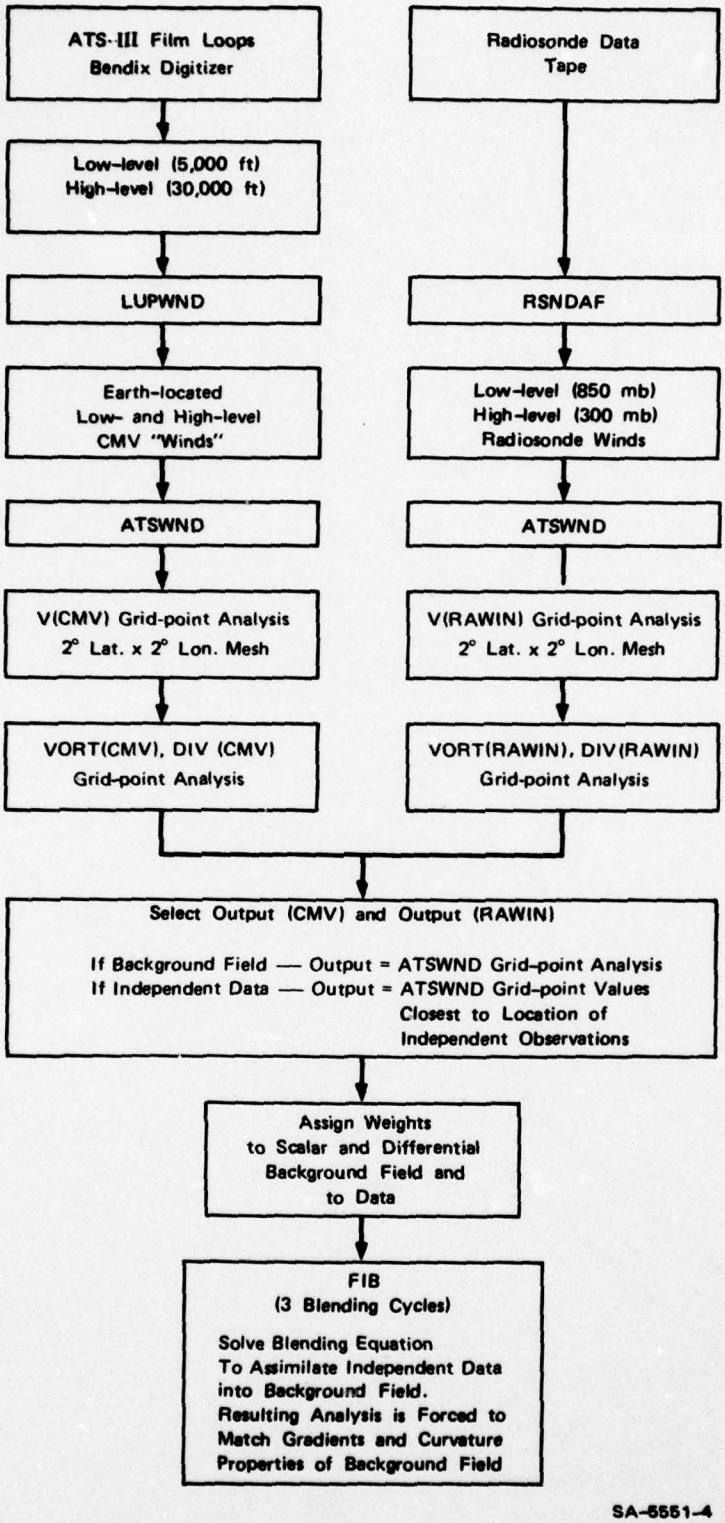

FIGURE 1 FLOW CHART SHOWING SEQUENCE OF DATA AND DATA ANALYSES INVOLVED IN THE FIB RESEARCH PROGRAM

IV CASE STUDIES CONDUCTED

A. General Plan and Methodology

As described in the previous section, SRI applied the FIB technique in the form of a comprehensive computer program supplied by NEPRF, which allowed for the processing, objective analysis, and subsequent blending of selected trial data sets. The program was executed on the data of two case studies, using SRI's CDC 6400 computer. The first case study was concerned with the passage of Hurricane Carmen across the Gulf of Mexico from the Yucatan Peninsula to the Louisiana Coast 2 through 8 September 1974. The second case study was concerned with the migration of an extra-tropical cyclone in the eastern North Pacific Ocean during the period 5 through 7 February 1976. Both areas are over water and conventional data for them are relatively sparse, so improvement in meteorological analyses could be expected from the assimilation of cloud motion data. Cloud motion winds were considered as the new, independent data to be blended with available conventional background analyses. Blending using relative vorticity and divergence computed from the cloud motion data was emphasized.

To evaluate the results obtained from the FIB technique for the first test case, a criterion was adopted based on the model low-level wind circulation associated with a tropical cyclone, wherein cyclonic relative vorticity and convergence in a circular area centered at the hurricane location increase significantly with decreasing radius. The criterion was applied by computing from the FIB analyses net relative vorticity and net divergence in rectangular areas of 14°, 10°, 6°, and 2° latitude × longitude centered at the location of Hurricane Carmen. The extent to which the computed values reproduced the magnitude and the relative variations of the adopted criterion was used as the standard for evaluating the FIB analyses.

A similar approach was used to evaluate the results of the second case study. A simplified form of the blending equation developed on the basis of the first case study results was executed on the data of the second case.

B. First Test Case Study

1. Scope

As already noted, the first case study was concerned with the passage of Hurricane Carmen across the Gulf of Mexico from the Yucatan Peninsula to the Louisiana Coast 2 through 8 September 1974. For this study ATS-3 cloud motion vector (CMV) winds and conventional radiosonde (RAWIN) winds were supplied by NEPRF.

Examination of the ATS-3 film loops from which the cloud motion vector end points were obtained by the Bendix digitizer technique showed that the initial CMV data, for 2 and 3 September, included grid registration errors that masked the explicit appearance of vortex circulation in the field of cloud motion winds around Hurricane Carmen. This vector error, when assumed to be spatially uniform, would not have affected the computed vorticity and divergence and the subsequent application of the FIB technique using these kinematic quantities. However, the error would have affected direct blending of the radiosonde winds and cloud motion vectors. Therefore, the FIB technique was not applied to any direct blending of wind vectors.

CMV winds were supplied in two height categories: "low-level," assigned to 5,000 ft, and "high-level," assigned to 30,000 ft. The radiosonde winds corresponding to these levels were assumed to be those of 850 mb and 300 mb. Only the low-level (850-mb) wind analyses were used. High-level (300-mb) cloud motion vectors were too few to allow meaningful grid-point analyses. Frequent time differences occurred between the ATS-3 satellite winds and the radiosonde data. As a rule, the cloud motion winds were blended with the closest synoptic-time radiosonde data.

2. Criterion for Evaluation of FIB Analyses

To evaluate the results obtained from the FIB technique for the first test case using the low-level VORT(CMV),* DIV(CMV) and the 805-mb VORT(RAWIN), DIV(RAWIN), a criterion was adopted based on the model low-level wind circulation associated with a tropical cyclone, wherein, on the scale of the FIB analyses, cyclonic relative vorticity and convergence in a circular area centered at the hurricane location increase significantly with decreasing radius. Figure 2 shows this criterion as derived from low-level vorticity and divergence computations made by Yanai (1961) in connection with a detailed analysis of typhoon formation and by Smith (1975) in connection with an analysis of Hurricane Celia (1970). Hawkins and Rubsam (1968) using aircraft winds at levels from 1000 mb to 700 mb computed values of cyclonic relative vorticity greater than 100×10^{-6} sec^{-1} within a 60-nmi radius of Hurricane Hilda (1964).

The criterion shown in Figure 2 was applied to the evaluation of the FIB analyses by computing net relative vorticity and net divergence in rectangular areas of 14°, 10°, 6°, and 2° latitude × longitude centered at the location of Hurricane Carmen. Figure 3 shows these concentric areas superposed on the ATSWND analysis of VORT(RAWIN) for 4 September, 12:00GMT. The extent to which the computed values of areal vorticity and divergence reproduced the magnitude and the relative variations shown in the data of Figure 2 was used as the standard for evaluating the FIB analyses. Specific quantitative evaluation criteria, such as vertical motion patterns in relation to radar-detected rain-band locations, were not considered applicable because of the limited coverage, reliability, and resolution of the data analyses.

3. Application of Evaluation Criterion to FIB Results

The FIB program was applied by blending the relative vorticity and divergence computed from the cloud motion vector and radiosonde data.

---

*In subsequent discussions, relative vorticity and divergence computed from cloud motion vectors and radiosonde winds are designated as, respectively, VORT(CMV), DIV(CMV) AND VORT(RAWIN), DIV(RAWIN).

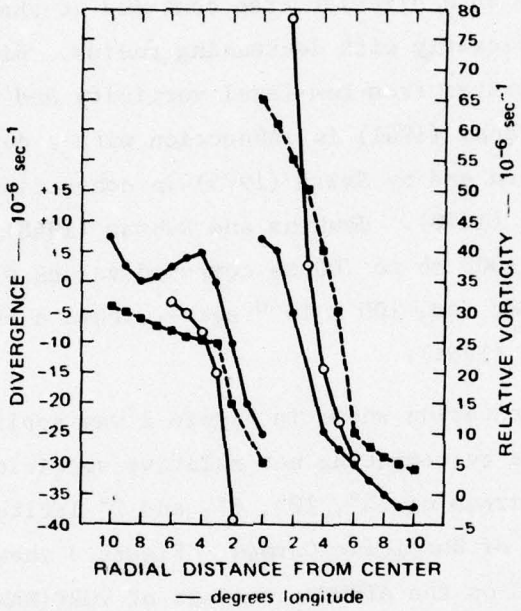

FIGURE 2 EXAMPLES OF INCREASE IN CYCLONIC RELATIVE VORTICITY AND CONVERGENCE IN A DIRECTION TOWARD THE CENTER OF A TROPICAL STORM, AS COMPUTED FROM WIND OBSERVATIONS BY YANAI (1961) and SMITH (1975)

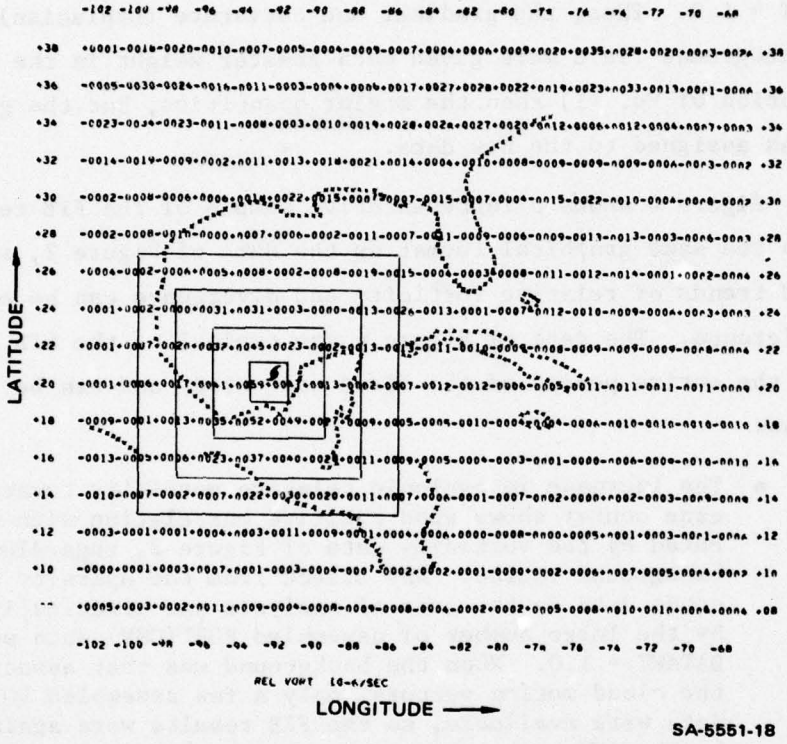

SA-5551-18

FIGURE 3 AREAS OF 14°, 10°, 6°, AND 2° (LATITUDE X LONGITUDE) FOR WHICH NET RELATIVE VORTICITY AND DIVERGENCE WERE COMPUTED TO EVALUATE *FIB ANALYSES FOR HURRICANE CARMEN*

Areas superposed on ATSWND analysis of relative vorticity from RAWIN, 4 September 1974, 12:00 GMT.

Two program options were considered. In one option, the cloud motion winds were selected as the independent data and were blended with a background field based on radiosonde winds. In the other, the radiosonde winds were assimilated in a background field based on the cloud motion data. Values for the weighting factors A through D in Eq. (1) were chosen as A = 0.001 and B through D = 0.01. At the grid points where new independent data were assembled, the weighting factor was set equal to DATAWT = 1.0. Thus, the gradient and curvature (Laplacian) properties of the background field were given much greater weight in the minimization solution of Eq. (1) than the scalar quantities, but the greatest weight was assigned to the new data.

Figure 4 shows a representative sample of the FIB results, presented in the same graphical format as the data of Figure 2, so that magnitudes and trends of relative vorticity and divergence can be evaluated by cross reference. The data of Figure 4 are typical of the FIB analyses made for the entire period of the first case study and can be summarized as follows:

- The increase in cyclonic relative vorticity toward the hurricane center shows good positive correlation with that indicated by the vorticity data of Figure 2, regardless of background choice. Any effect from the sparsity of rawinsonde data in the area of analysis was practically eliminated by the large number of assembled VORT(CMV) data weighted by DATAWT = 1.0. When the background was that associated with the cloud motion vectors, only a few assembled VORT(RAWIN) data were available, so the FIB results were again dominated by the CMV background data. Thus, the CMV data always controlled the FIB analyses, regardless of background choice, because of the dense CMV data coverage in an area of sparse radiosonde data.
- The FIB analyses of divergence reflect unrealistic values. Neither the sign of the divergence nor its trend corresponds to the standard of Figure 2. The discrepancy results from bad values of divergence associated with the initial CMV data. Application of these values to the FIB program introduces meteorologically unacceptable effects into the solution of the blending equation.
- Unless the cloud motion vectors are obtained with higher accuracy and better height discrimination, only their rotational part can be reliably included in the FIB analysis; that is, only blending using vorticity derived from the cloud motion vectors gives meteorologically significant results.

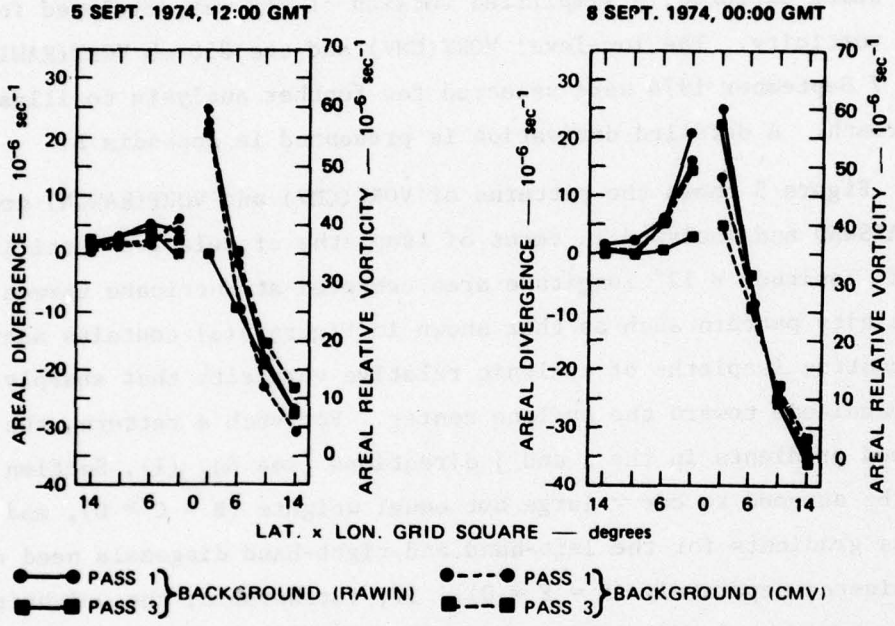

FIGURE 4 SAMPLE OF FIB ANALYSES FOR THE FIRST TEST CASE, PRESENTED IN TERMS OF EVALUATION CRITERION OF FIGURE 2

FIB program was applied by utilizing vorticity and divergence computed from V (CMV) and V (RAWIN) with different background fields and DATAWT = 1.0, A = 0.001, B, C, D, E, F = 0.01.

More details of the results obtained from the application of the FIB program to the data of the first test case study are presented in Appendix A.

C. Simplified Blending Equation

While the dependence of the FIB results for the first study case on independent data weight (DATAWT) and on background gradient weights (B-F) was being explored, a simplified version of FIB was developed for blending vorticity. The low-level VORT(CMV) and the 850-mb VORT(RAWIN) data for 7 September 1974 were selected for further analysis to illustrate the approach. A detailed derivation is presented in Appendix B.

Figure 5 shows the patterns of VORT(CMV) and VORT(RAWIN) generated by ATSWND and analyzed in terms of isopleths of relative vorticity within a 12° latitude × 12° longitude area centered at Hurricane Carmen. A vorticity pattern such as that shown in Figure 5(a) contains near-concentric isopleths of cyclonic relative vorticity that sharply increase in magnitude toward the cyclone center. For such a pattern, the background gradients in the i and j directions [see Eq. (1), Section III-B] can be assumed to carry large but equal weights ($B = C \gg 0$), and the cross gradients for the left-hand and right-hand diagonals need not be considered separately ($E = F = 0$). If, furthermore, the weighting factors are assigned without spatial variability, the blending equation can be simplified to a form that comprises only blending parameters related to the Laplacian properties at i,j and at four surrounding grid points. Thus, the curvature of the vorticity isopleths at i,j and at adjacent grid points are the blending parameters. In this case, four weighting factors were assigned: A, $B \equiv C \equiv W$, D, and DATAWT (for a detailed discussion, see Appendix B).

Figure 6 shows the sensitivity of the FIB analysis of the relative vorticity [VORT(FIB)] to different values of $B \equiv C \equiv W$, using VORT(RAWIN) of Figure 5(a) as the background field with $A = 0.001$ and $D = 0$, and VORT(CMV) of Figure 5(b) as the independent data with weight DATAWT = 1.0. Each curve represents VORT(FIB) as a function of W (from W = 0.01 to W = 1.0) at a grid point where VORT(CMV) data were assembled. The ten grid-point

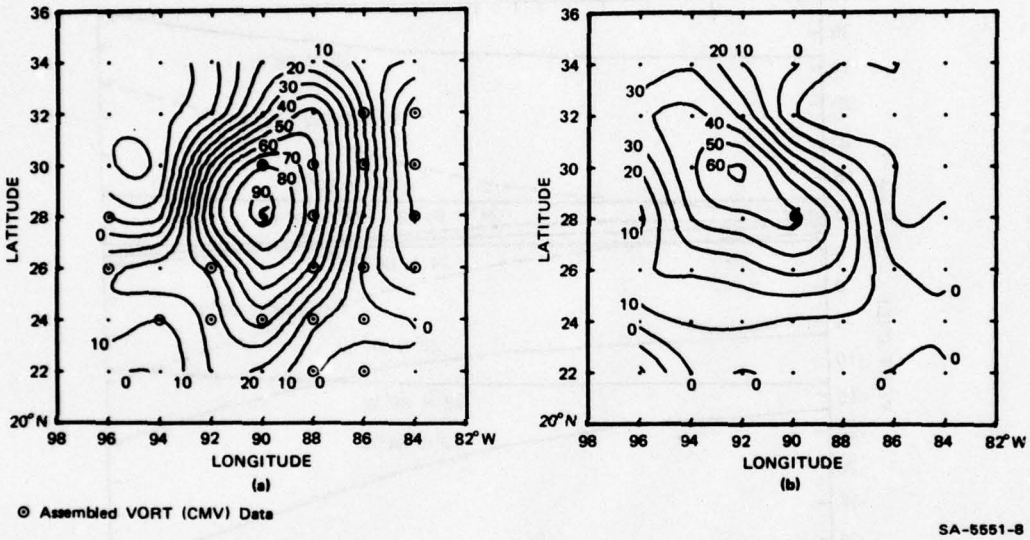

FIGURE 5 ISOPLETHS OF RELATIVE VORTICITY (10^{-6} sec^{-1}) SHOWING VORTICITY PATTERNS ASSOCIATED WITH HURRICANE CARMEN AS ANALYZED FROM (a) BACKGROUND FIELD OF 850-mb VORT(RAWIN), 8 SEPTEMBER 1974, 00:00 GMT; (b) INDEPENDENT DATA FIELD OF LOW-LEVEL VORT(CMV), 7 SEPTEMBER 1974, 18:47-21:10 GMT

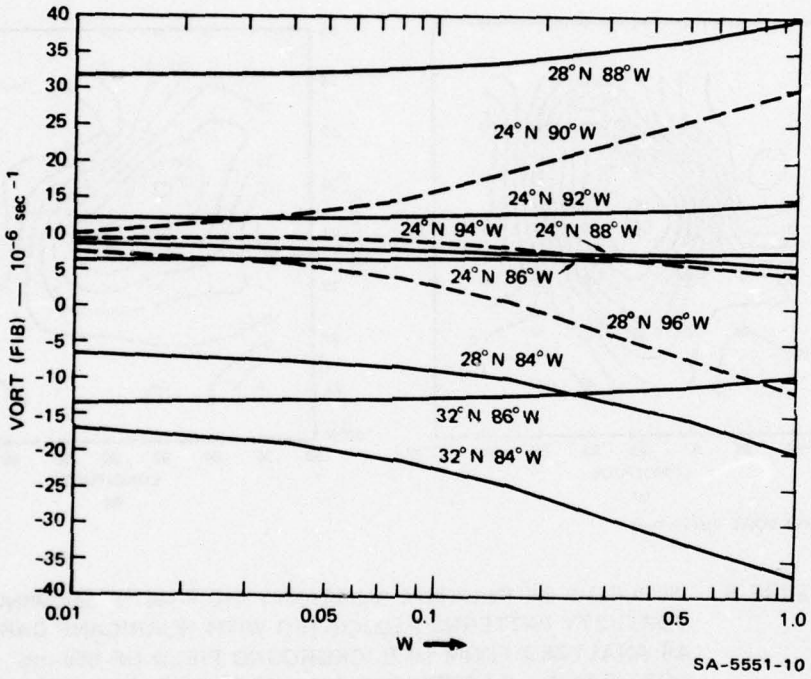

FIGURE 6 VALUE OF VORT(FIB) AS A FUNCTION OF W FOR 10 GRID-POINTS [SEE FIGURE 5(a)] AT WHICH VORT(CMV) DATA WERE ASSEMBLED USING A = 0.001 AND DATAWT = 1.0

locations in the VORT(RAWIN) background field can be identified by reference to Figure 5(a). It can be seen that significant changes in VORT(FIB) require rather large values of W, unless the grid point is associated with relatively large curvature in the background vorticity isopleths, as occurs, for example, at 24°N, 90°W and at 28°N, 96°W. In general, increasing W = 0.01 by a factor of 10 to 20 does not result in significant changes in VORT(FIB). Values of W nearly equal to the data weight DATAWT are required to conserve the curvature characteristics of the background vorticity field.

Small values of W would affect the VORT(FIB) analysis much more than shown in Figure 6 if DATAWT were reduced proportionally. It is the value of W relative to that of DATAWT which influences the FIB analysis. For example, Figure 6 would remain unchanged if DATAWT and W were divided by the same factor, provided DATAWT remained large relative to A = 0.001.

In practice, when applying FIB to the blending of vorticity, the simplified blending equation can be used, and a proper choice of DATAWT and W can be made semiobjectively by (1) examining the initial fields of VORT(RAWIN) and VORT(CMV) generated by ATSWND, to determine the extent to which the background patterns should be conserved, and (2) computing the background Laplacian field and determining the values of W relative to DATAWT at which VORT(FIB) begins to change significantly.

D. Second Test Case Study

1. Scope

A second case study to test and evaluate the FIB technique was concerned with the migration of an extratropical cyclone in the eastern North Pacific Ocean during the period 5 through 7 February 1976. Earth-located CMV data obtained from the Space Science and Engineering Center of the University of Wisconsin were available as part of a NASA/NOAA-sponsored Data Systems Test (DST-6). Cloud motion winds were generated on the McIDAS from SMS-2 data. The background with which the independent CMV data must be blended was the geostrophic wind field obtained from the Fleet Numerical Weather Central (FNWC) constant-pressure height

analyses for the levels and times closest to the heights and times of the CMV data. The geostrophic winds as a function of latitude and longitude provided the input to ATSWND, which, subsequently, generated the background fields of wind, vorticity, and divergence on a 2° latitude × 2° longitude grid mesh.

In view of the good representation of the rotational wind field by the cloud motion data of the first case study, the FIB technique was applied by blending CMV winds and geostrophic winds, using the respective vorticity properties. In this case, the simplified blending equation was used, and weighting factors were assigned according to A = 0.001; DATAWT = 1.0; B = C = 1.0; D = E = F = 0. The choice of B = C = 1.0 forced the vorticity-isoline patterns in the FIB analyses to conform to those associated with the background (see Figure 6). Divergence obtained from the CMV data was evaluated, but assimilation in a background field based on geostrophic winds was not attempted, because of the nonrepresentativeness of the geostrophic divergence. Blending was carried out by using both low-level and high-level winds. Uncertainties related to time and possible height differences between the CMV and RAWIN data must be considered in interpreting the results of the data blending.

2. Application of FIB Program

Data blending was carried out for 6 and 7 February 1976, 00:00 GMT and 12:00 GMT, and for 8 February 00:00 GMT. Since the FIB technique and the blending procedure showed similar results for these five cases, the salient features of the second test study can be adequately discussed on the basis of a single case. The single case valid for 6 February 1976, 00:00 GMT, was selected as representative. Figure 7 shows the SMS-2 infrared cloud images in the area of the second case study for 5 February 1976, 21:45 GMT, and the location and height levels of corresponding CMV winds obtained during the period 22:45-23:45 GMT. The differences in coverage between low-level (900-mb) and high-level (200- and 300-mb) CMV data are evident. High-level cloud motions are restricted to the most western and southeastern parts of the analysis area. The low-level motions having dense coverage around the center of the extratropical cyclone are emphasized in the following analyses.

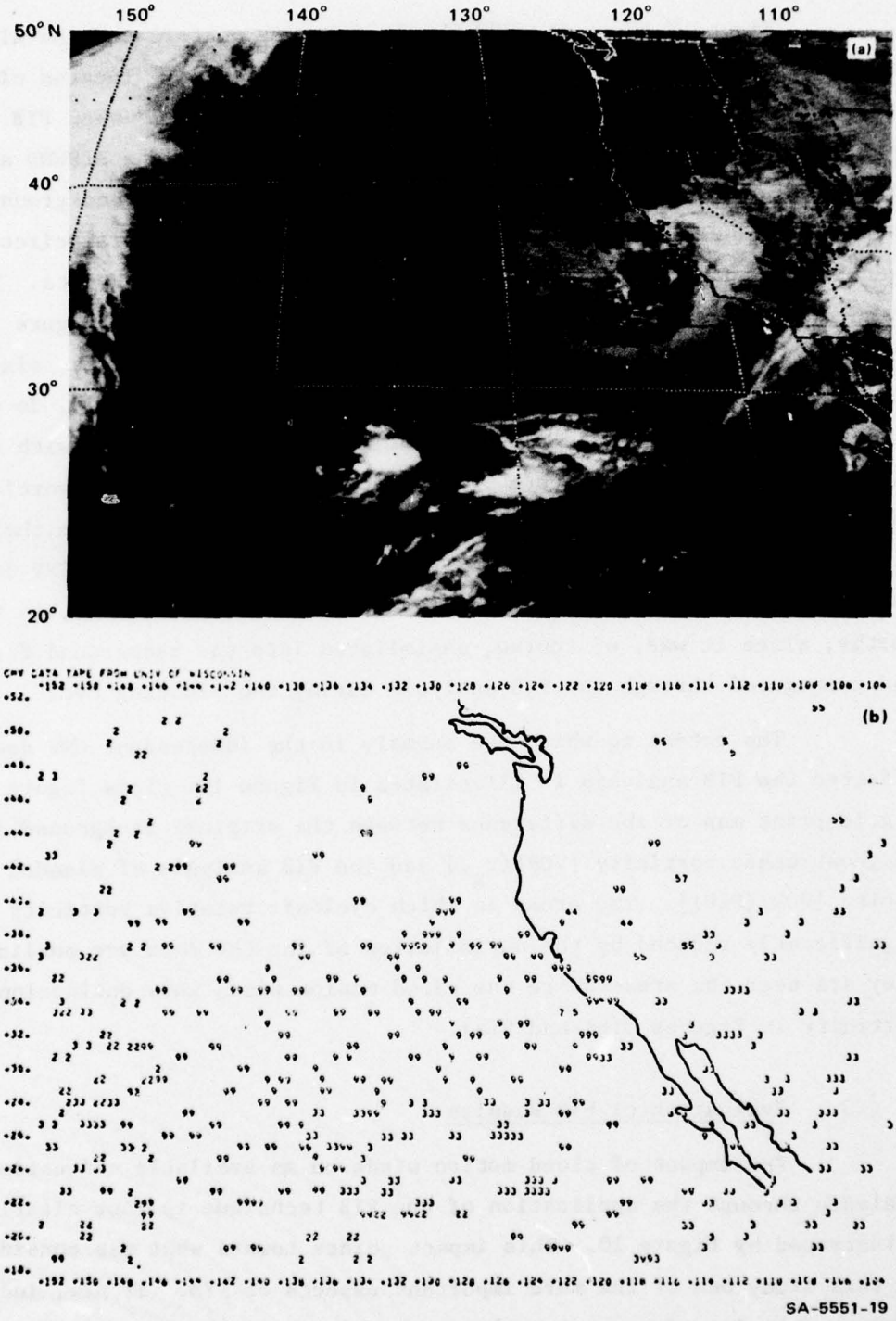

FIGURE 7 EXAMPLE OF SMS-2 DATA COVERAGE IN AREA OF SECOND TEST CASE STUDY (a) INFRARED CLOUD IMAGES, 5 FEBRUARY 1976, 21:45 GMT; (b) CLOUD MOTION VECTOR LOCATIONS, 5 FEBRUARY 1976, 22:45-23:45 GMT
Numbers identify cloud motion heights in hundreds of millibars.

Figure 8 shows the 900-mb cloud motion vectors and the ATSWND-generated grid-point analyses obtained from the randomly located cloud motion winds and from the FNWC 850-mb geostrophic winds. When FIB was applied, the independent information was obtained from the ATSWND analysis of the CMV data, while the geostrophic winds provided the background field. In general, there was very good agreement between the general circulation features of the FNWC analysis and those outlined by the CMV data. There were, however, some important differences. For example, in Figure 8(b) in a small area near 32°N, 119°W, the cloud motion winds differ significantly from the geostrophic background field, and, intuitively, do not seem to fit the synoptic-scale circulation pattern associated with the extratropical cyclone. Figure 9 shows the fields of relative vorticity computed from the CMV winds of Figure 8(b) [VORT(CMV)] and from the geostrophic winds of Figure 8(c) [VORT(V_g)]. The anomaly in the CMV data, which is very evident in the vorticity analysis of Figure 9(a), is noteworthy, since it was, of course, assimilated into the background field and propagated through the FIB analysis during the blending cycle.

The extent to which the anomaly in the independent CMV data affected the FIB analysis is illustrated in Figure 10. This figure shows a grid print map of the difference between the original background field of geostrophic vorticity [VORT(V_g)] and the FIB analysis of blended vorticity [VORT(FIB)]. The areas in which cyclonic relative vorticity was significantly reduced by the assimilation of the CMV data are outlined. They are near the areas where the cloud motion winds show anticyclonic vorticity in Figures 8(b) and 9(a).

3. Evaluation of FIB Results

The impact of cloud motion winds on an available conventional analysis through the application of the FIB technique is most clearly illustrated by Figure 10. This impact points toward what was considered in this study one of the more important aspects of FIB. If new, independent data introduce an anomaly in the blended analysis product, the FIB program includes a routine, called Weight Reevaluation, which enables reexamination of each blended datum value to assess its disparity with the

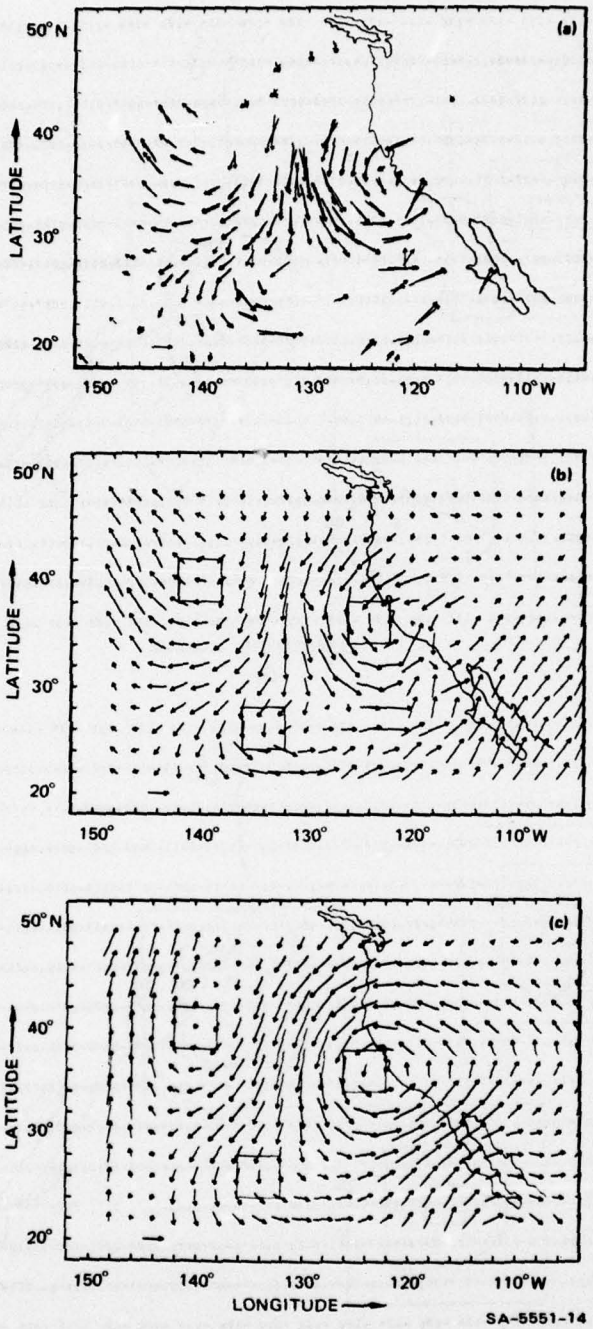

FIGURE 8 DATA ANALYSES USED TO INITIALIZE FIB TECHNIQUE FOR SECOND CASE STUDY: (a) 900-mb CMV COVERAGE (SMS-2, 5 FEBRUARY 1976, 22:45-23:45 GMT); (b) INDEPENDENT DATA, ATSWND ANALYSIS OF CMV WINDS; (c) BACKGROUND DATA, ATSWND ANALYSIS OF FNWC 850-mb GEOSTROPHIC WINDS (6 FEBRUARY 1976, 00:00 GMT)

Boxes indicate major circulation centers in FNWC analysis.

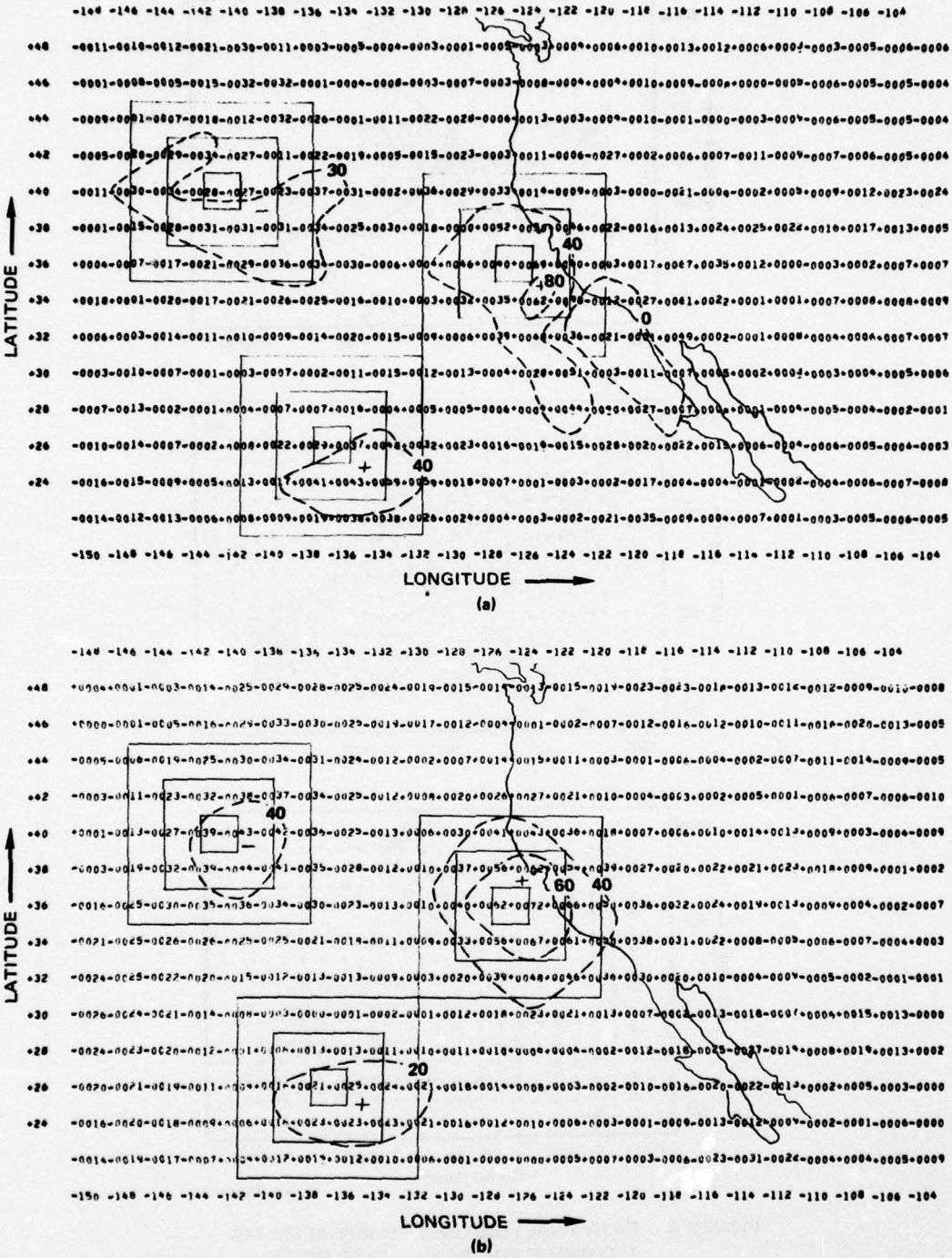

FIGURE 9 ATSWND ANALYSES OF RELATIVE VORTICITY (10^{-6} sec^{-1}) OBTAINED FROM (a) 900-mb CMV WINDS (5 FEBRUARY 1976, 22:45–23:45 GMT) (b) FNWC 850-mb GEOSTROPHIC WINDS (6 FEBRUARY 1976, 00:00 GMT)

Boxes indicate major circulation centers; dashed isopleths indicate relative vorticity patterns.

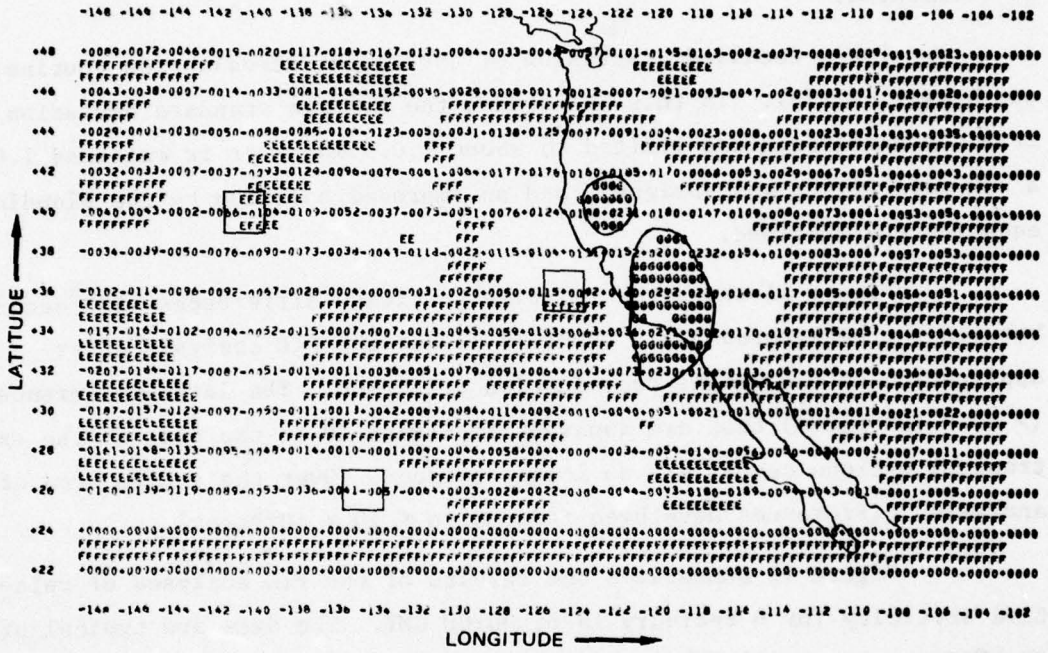

FIGURE 10 RELATIVE VORTICITY DIFFERENCE (10^{-7} sec^{-1}) BETWEEN ORIGINAL BACKGROUND FIELD AND FIB ANALYSIS [VORT (V_g)-VORT(FIB)]

Note large reduction in background vorticity in area of extratropical cyclone. Machine contouring denotes: E = < - 10.0 x 10^{-6} sec^{-1}; F = 0 to + 10.0 x 10^{-6} sec^{-1}; G = > + 20.0 x 10^{-6} sec^{-1}.

background. By setting a limit on the extent to which the blended analysis can differ from the background, large disparities such as those illustrated in Figure 10 near the extratropical cyclone can be suppressed by reducing the weights (DATAWT) of the independent data at relevant grid points and recycling the data through the blending technique. The constraining criterion that is programmed into the FIB technique can be relaxed or tightened, depending on whether the anomaly must be maintained or eliminated.

For a detailed discussion of the Weight Reevaluation routine, see Maxwell (1976). In this SRI study, the average standard deviation from the background was limited to about 1.0. Whenever it exceeded 1.0, a new data weight was assigned, and an improved solution to the blending equation was obtained.

Figure 11 shows the relative vorticity differences ($10^{-7}sec^{-1}$) between the background field [VORT (V_g)] and the FIB analysis after application of the weight reevaluation criterion. The large differences ($> 20 \times 10^{-6}sec^{-1}$) that are apparent in Figure 10 to the east of the extratropical cyclone center are no longer present. Over the entire area of analysis, differences have been reduced to $\ll 10 \times 10^{-6}sec^{-1}$.

Figure 12 summarizes the results of the FIB analyses of relative vorticity for 6 February 1976, 00:00 GMT. The data are typical of the FIB results obtained from the second case study. The blending technique was applied by using both low-level and high-level cloud motion winds. As already noted, a criterion similar to that applied in the first case study was used for evaluation. Figure 12 represents magnitudes and trends of net relative vorticity computed over variable-mesh-size concentric grid boxes centered at the three circulation systems (extratropical cyclone, anticyclone, and sharp trough) indicated in Figures 8 and 9. For all three systems, the initial impact of the cloud motion winds on the magnitude of the background vorticity field [VORT(BACKGROUND) vs. VORT(FIB)] can be seen to be significant. When the criterion of keeping the analysis product within one standard deviation of the background is applied, the FIB analysis conforms much more to the background.

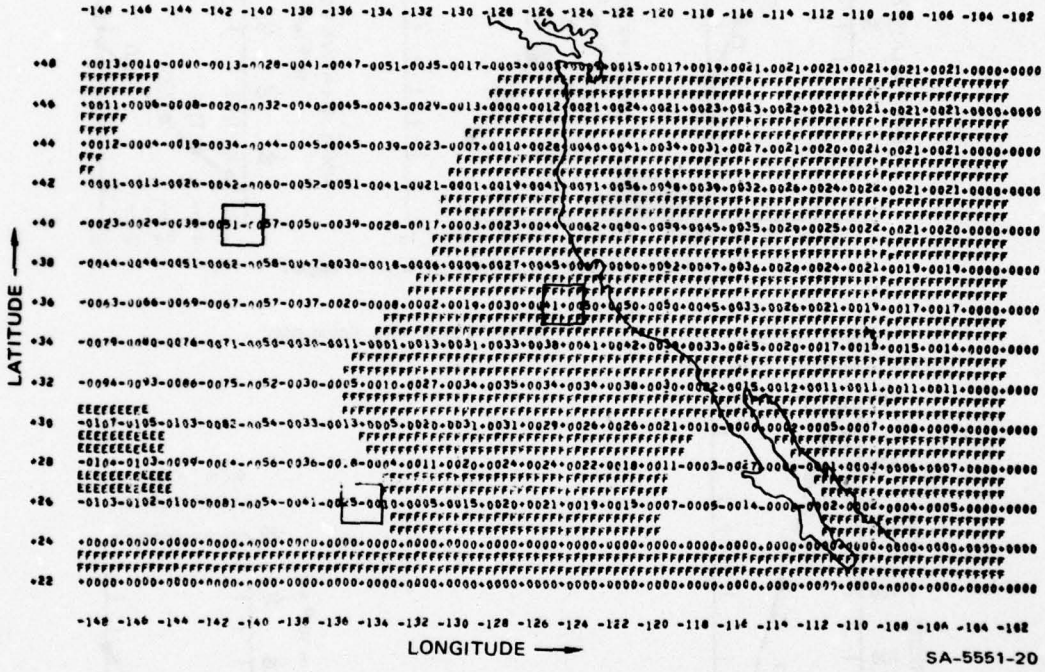

FIGURE 11 RELATIVE VORTICITY DIFFERENCE (10^{-7}sec^{-1}) BETWEEN ORIGINAL BACKGROUND FIELD AND FIB ANALYSIS, AFTER WEIGHT REEVALUATION [VORT(Vg)-VORT(FIB AFTER WEIGHT REEVALUATION)].

Note reduction of large differences in area of extratropical cyclone. Machine contouring denotes: E = <-10.0 X 10^{-6} sec^{-1}; F = 0 to + 10.0 X 10^{-6} sec^{-1}.

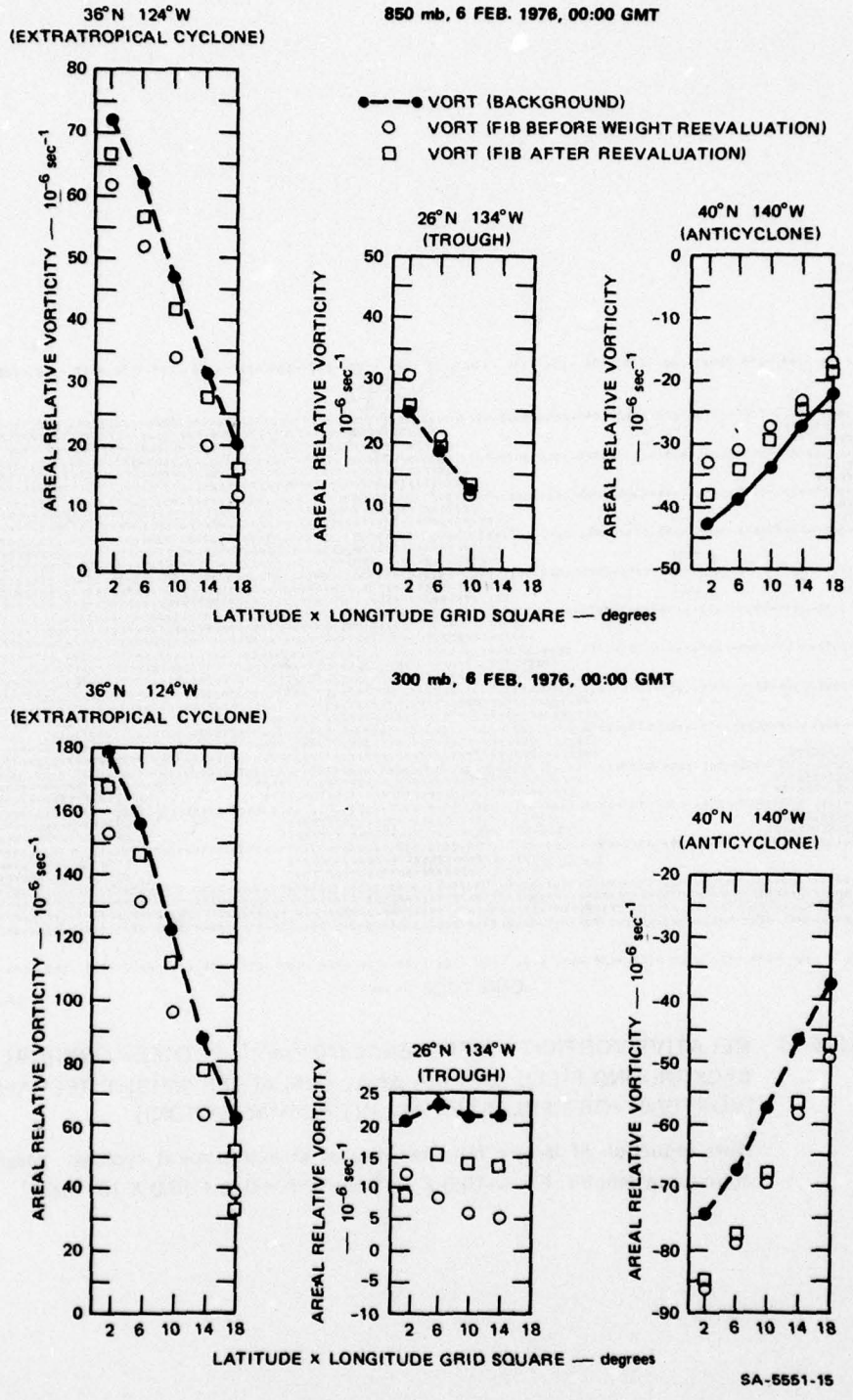

FIGURE 12 SAMPLE OF FIB ANALYSIS RESLULTS FOR THE SECOND TEST CASE, PRESENTED IN TERMS OF MAGNITUDES AND TRENDS OF NET RELATIVE VORTICITY COMPUTED OVER GRID BOXES CENTERED AT THREE CIRCULATION SYSTEMS

FIB was executed using DATAWT = 1.0, A = 0.01, B = C = 1.0, E = F = D = 0.

Vorticity trends with respect to the center of the system are realistic because of the relatively large weights assigned to the curvature of the background vorticity isopleths (B = C = 1.0).

The meteorological significance of the absolute values of vorticity in the FIB analyses is difficult to assess, since the true vorticity characteristics of the atmospheric circulation systems were not known. It is apparent, however, that the FIB program allows, by manipulation of the background weights and the weight reevaluation criterion, for any control the user wants to impose on the degree of change introduced by the cloud motion winds.

E. An Alternative Method for Analyzing Cloud Motion Vectors

To aid in evaluating the accuracy and efficiency of the FIB technique, we experimented with an alternative method. In this approach, the product is a blended grid-point wind analysis, rather than a blended vorticity analysis (as described earlier). The alternative method is presented because:

- It readily provides grid-point wind analysis in a form appropriate for input to a numerical prediction model while reducing computer time by a factor of nearly 3 compared to the FIB technique.
- It can easily generate a cloud motion data/conventional data wind analysis in terms of its nondivergent (rotational) part. Current difficulties in determining reliable divergence patterns from cloud motion data may require that the wind analysis be made nondivergent.
- It is available within the NEPRF-supplied computer programs by combining Subroutines GRAN and BALDV in the ATSWND element.

The alternative method makes use of the excellent quality of the pressure-height analyses produced by FNWC, by computing geostrophic winds from them and using the geostrophic u and v wind components as background (that is, a first-guess field) in an objective analysis of the cloud motions. The weights assigned to the first guess is so chosen that the first guess is retained in areas devoid of cloud motion vectors, but has

little influence where cloud motion vectors are numerous. In the latter areas, each grid-point value of wind is a weighted average of several nearby cloud motion vectors. The analysis method is a statistical one that fits a first-degree polynomial by least squares to several observations near the grid point. (The basic form has been described by Endlich and Mancuso, 1968, and Mancuso and Endlich, 1973.) The weighting function for an observation is decreased with its distance from the grid point, as is normally done. In addition, the weight is made to reflect the orientation of the observed cloud motion vector and grid point in relation to the local flow direction, so that upstream-downstream observations have greater weight than cross-stream observations at the same distances, especially in regions of strong flow. In our experience, this is an important feature in giving realistic, elongated isotach fields. The merit of this type of anisotropic weighting was discussed theoretically by Sasaki (1971).

In the computer routines used in this study the objective wind analysis procedure is called GRAN. The number of wind observations used in computing a grid-point wind component is a parameter (KS) that must be specified before calling GRAN. In analyzing radiosonde winds, a value of KS of 5 or 6 has been found to be appropriate. Since the present cloud motion vectors come in pairs [as shown, for example, in Figure 8(a)], KS was set equal to 12 (six pairs); this value gave good results. A smaller value of KS would give greater emphasis to individual winds near a grid point, and a less smooth analysis. A second computer routine that is useful in wind analysis enables one to alter the vorticity or divergence fields (Endlich, 1967). For example, one can alter grid-point u and v components to make them nondivergent. This routine is called BALDV.

The results of using this alternative method to analyze cloud motion vectors are illustrated by using the data for 6 February 1976, 00:00 GMT. The geostrophic wind vectors at 850 mb computed from the FNWC height data have been shown in Figure 8(c). The analysis has good resolution and an excellent overall appearance. In general, the low-level cloud motion vectors shown in Figure 8(a) agree well with the geostrophic vectors. However, the low-level cloud motion vectors are not evenly distributed

over the region. To the east of the low-pressure center, satellite IR photographs showed that the clouds were generally at middle or high levels; thus no low-level motions were measured. Also, at 34°N, 120°W, a southwesterly cloud motion vector appears to be of significantly higher speed than its neighbors; and, at approximately 28°N, 120°W, a cloud motion vector is nearly at right angles to its neighbors. This vector was probably unrepresentative or was assigned to the wrong altitude. These anomalous features were evident in the FIB analyses; they could be suppressed by proper adjustment of the weighting factors. The alternative method also has the ability to suppress these anomalies.

Figure 13(a) shows a grid-point wind analysis obtained by applying the alternative method to the low-level CMV data [Figure 8(a)], using the FNWC 850-mb geostrophic winds as a first-guess field. [The geostrophic vectors are shown in Figure 13(c).] There is some unevenness in the winds in the area east of the low, where the CMV coverage was originally poor. (This unevenness appeared as small patterns of positive and negative divergence (not shown) computed from the grid-point winds.) In general, it was found that the divergence patterns associated with Figure 13(a) did not relate well to the clouds; therefore it seemed desirable to make the wind analysis nondivergent, while leaving its vorticity unchanged. This was done by using Subroutine BALDV. The results are shown in Figure 13(b). This nondivergent vector field appears quite similar to the geostrophic wind field of Figure 13(c). However, differences between the relative vorticities of the two fields are appreciable, as illustrated by the isolines in Figure 13(c). Positive values indicate that the objective analysis has larger positive (cyclonic) vorticity than the geostrophic analysis, and negative values indicate the reverse. The objective analysis method produces larger cyclonic vorticity for the trough to the southwest of the low center, and also for the entire southeast quadrant of the extratropical cyclone. To the north of the cyclone center, there is more anticyclonic vorticity in the objective analysis. Whether these vorticity differences are realistic or not cannot be determined for certain, since there are no independent data to enable this evaluation to be made.

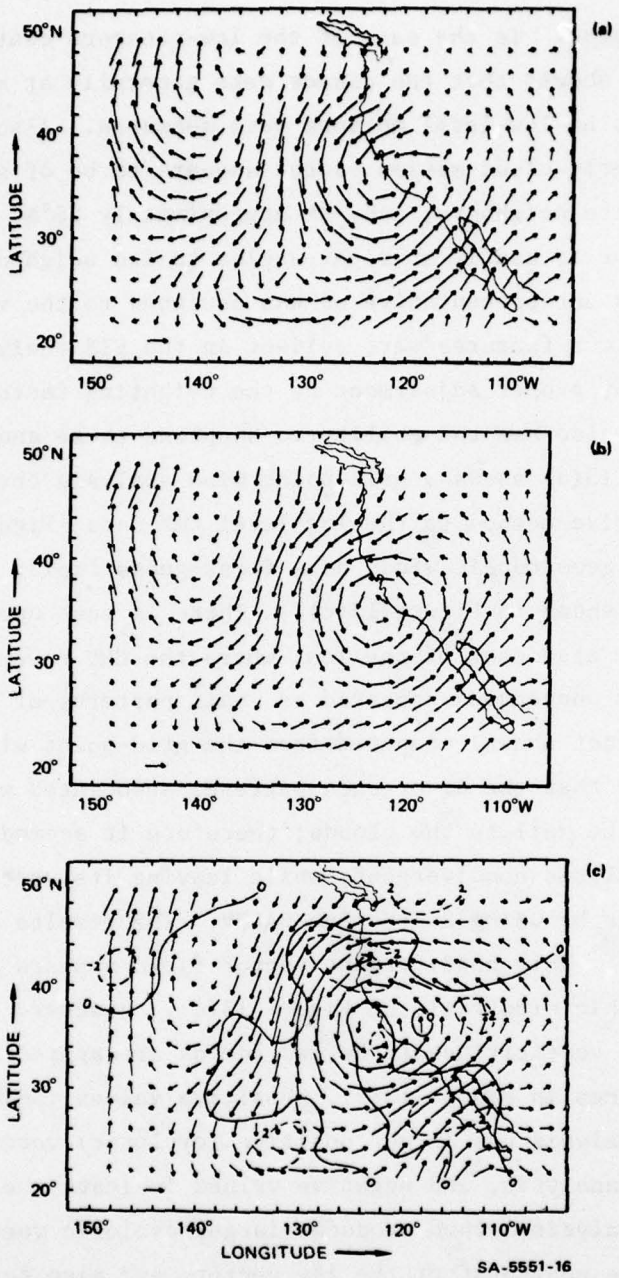

FIGURE 13 RESULTS FROM ALTERNATIVE OBJECTIVE ANALYSIS TECHNIQUE

(a) OBJECTIVE ANALYSIS OF CMV DATA (5 FEBRUARY 1976, 22:45-23:45 GMT) USING FNWC 850-mb GEOSTROPHIC WIND FIELD (6 FEBRUARY, 1976 00:00 GMT) AS A FIRST GUESS

(b) ROTATIONAL (NONDIVERGENT) VECTOR FIELD ASSOCIATED WITH (a)

(c) ISOLINES OF THE DIFFERENCE (10^{-5} sec^{-1}) BETWEEN THE VORTICITY OF THE OBJECTIVE ANALYSIS (b) AND THE FNWC GEOSTROPHIC VORTICITY, SUPERIMPOSED ON THE GEOSTROPHIC WIND VECTORS

In summary, the alternative method of analysis uses the conventional data, in the form of geostrophic winds obtained from the FNWC height fields, as a background for directly analyzing cloud motion vectors. Although the general appearance of the analyzed cloud motion vectors and that of the geostrophic vectors is very similar, there are significant differences in the vorticity fields, particularly in regard to the smaller-scale (subsynoptic) troughs and ridges. Presumably, these differences would be important for a limited-area fine-mesh numerical forecasting model, although they are probably not important for a global model. On the other hand, the divergence fields computed from these cloud motion vectors were not reliable; therefore, the analysis of cloud motion vectors was made nondivergent.

V CONCLUSIONS AND RECOMMENDATIONS

Conclusions and recommendations are based on the results obtained by executing FIB on the data of the two case studies discussed previously and described in more detail in Appendices A, B, and C.

A. General

The FIB program and its associated elements as organized and developed by NEPRF are suitable for blending satellite-derived cloud motion data with conventional wind information, and they can provide meteorologically meaningful analyses. Quality control of the cloud motion winds, however, must be exercised. Execution of the program requires judgment as to whether features in the cloud motion data that appear anomalous with respect to the available conventional-data analysis should be maintained or suppressed in the blending cycle. By manipulation of built-in constraints, the FIB program can accept, suppress, or reject undesirable features.

This study suggests that subjective interaction with the computer program is required, to set the proper constraints on the degree of change allowed in the resultant FIB analysis. Initial input data and intermediate steps in the FIB program need to be monitored as long as the true relation of cloud motion vectors to the atmospheric wind field cannot be objectively formulated.

B. Specific

For both case studies, the FIB program properly executed the blending of information obtained from cloud motion winds with that available from conventional data. It was found that, when blending using vorticity is applied, a simplified form of the blending equation can be used that considers only the Laplacian (curvature) properties of the background field as the blending parameter. In this case, the weight of the independent data (DATAWT) should be set nearly equal to the weight of the background Laplacian.

The significance of the FIB analyses was found to depend entirely on the information content of the cloud motion winds. For the first case study, only the blending that used vorticity derived from the cloud motion vectors gave meteorologically significant results; that is, only the rotational part of the cloud motion vector could be reliably included in the FIB technique. Divergence computed from the CMV data of the first test case study, and its subsequent assimilation through the FIB program, did not provide meteorologically acceptable analyses. The results from the second case study were similar. Circulation was again the outstanding feature in the CMV data that provided meteorologically significant input into the FIB technique. Divergence computed from the cloud motion winds was evaluated but not used in the FIB program because of the non-representativeness of the divergence computed from the geostrophic wind.

The following blending technique is tentatively recommended as optimum:

Step 1--Apply the FIB program using VORT(CMV) as independent data and VORT(RAWIN) as initial background field.

Step 2--Apply the ATSWND Subroutine BALDV to convert VORT(FIB) to its corresponding (purely rotational) vector field.

Step 3--Apply the ATSWND Subroutine BALDV to the background field of DIV(RAWIN) to obtain the corresponding (purely divergent) vector field.

Step 4--Add the vector fields obtained under Steps 2 and 3 to obtain a final analysis product that represents a vector wind field improved over the initial background wind field with respect to its rotational properties only. Its irrotational (divergent) part will remain that associated with the initial background field.

This recommended blending technique can also be carried out by an alternative objective analysis method that can be readily assembled by using subroutines available in the NEPRF computer program.

A crucial and unresolved problem is that of determining divergence fields from satellite cloud motion data for input to fine-mesh forecasting models. In this study, divergence objectively computed from the ATSWND analysis of "low-level" and "high-level" cloud motion winds was not realistic. It is emphasized, however, that reliable evaluation of divergence entails a three-dimensional analysis, which was considered outside

the scope of the study. If divergence computed from cloud motion winds is to be evaluated more rigorously as to its meteorological significance and operation usefulness, it is recommended that divergence fields be obtained at five or six levels from 1000 mb to 100 mb and that the objective procedure described by O'Brien (1970) and Frankhauser (1969) be applied to adjust the vertical profile of divergence so that realistic boundary conditions of vertical motion at 1000 mb and 100 mb are satisfied. The cloud motion wind field can, subsequently, be adjusted at all levels to reflect the adjustments in divergence.

Also, a promising approach is to use satellite microwave radiometer measurements that show moisture concentrations, to compute the low-level convergence necessary to account for these concentrations, and to alter the cloud motion vector analysis to fit the specified convergence, using Subroutine BALDV (Viezee, 1977).

Appendix A

FIRST TEST CASE ANALYSES

Appendix A

FIRST TEST CASE ANALYSES

1. General

The first test case considered the passage of Hurricane Carmen across the Gulf of Mexico from the Yucatan Peninsula to the Louisiana Coast, 2 through 8 September 1974. Successive locations are indicated in Figure A-1. Observations from the conventional radiosonde network and cloud

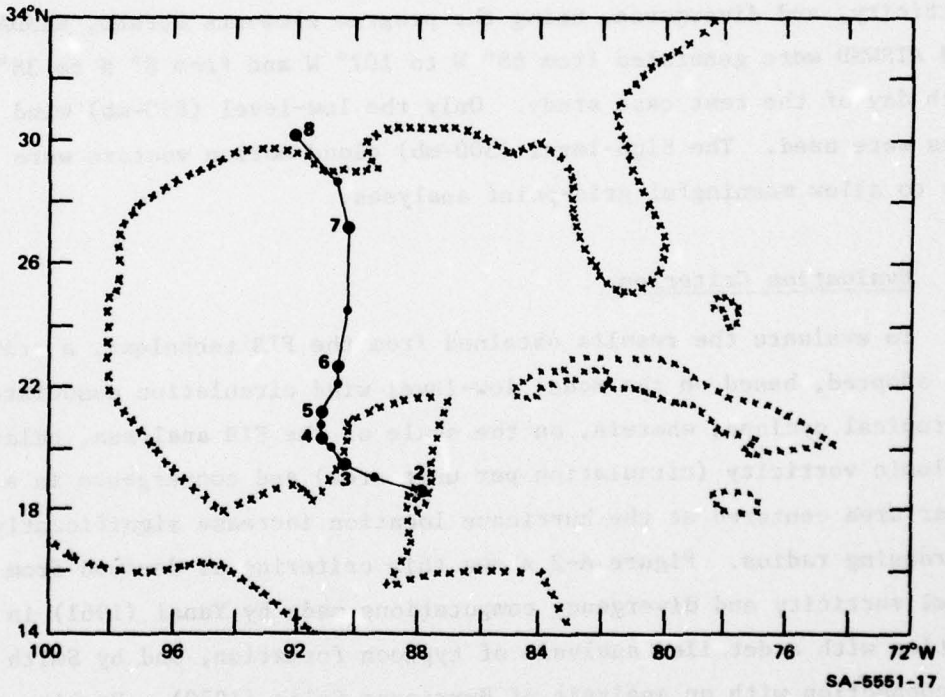

FIGURE A-1 TRACK OF TROPICAL STORM (HURRICANE) CARMEN FROM 2 TO 8 SEPTEMBER 1974

● 12:00 GMT
• 00:00 GMT

motion winds from the ATS-3 satellite were supplied by NEPRF. Cloud motion vector endpoints obtained by means of the interactive man-movie loop-Bendix Digitizer technique were supplied in two height categories: "low-level," assigned to 5,000 ft, and "high-level," assigned to 30,000 ft. The radiosonde winds corresponding to these levels were assumed to be those of 850 mb and 300 mb. In addition to the required height matching, frequent time differences of 3 to 4 hours occurred between the ATS-3 satellite wind data and the radiosonde data. The computer programs did not contain an algorithm to account for such time differences. As a rule, the cloud motion winds were blended with the closest synoptic-time radiosonde data. Uncertainties related to time and height differences must be considered in interpreting results of the data blending.

Two-degree latitude-longitude grid-mesh analyses of wind, relative vorticity, and divergence, using the program elements LUPWND, RSNDAF, and ATSWND were generated from 68° W to 102° W and from 8° N to 38° N, each day of the test case study. Only the low-level (850-mb) wind analyses were used. The high-level (300-mb) cloud motion vectors were too few to allow meaningful grid-point analyses.

2. Evaluation Criterion

To evaluate the results obtained from the FIB technique, a criterion was adopted, based on the model low-level wind circulation associated with a tropical cyclone, wherein, on the scale of the FIB analyses, relative cyclonic vorticity (circulation per unit area) and convergence in a circular area centered at the hurricane location increase significantly with decreasing radius. Figure A-2 shows this criterion as derived from low-level vorticity and divergency computations made by Yanai (1961) in connection with a detailed analysis of typhoon formation, and by Smith (1975) in connection with an analysis of Hurricane Celia (1970). Hawkins and Rubsam (1968) using aircraft winds computed values of relative cyclonic vorticity greater than 100×10^{-6} sec^{-1} within a 60-nmi radius of Hurricane Hilda (1964). Table A-1 presents further data in support of the convergence criterion. The listed values of net divergence computed from

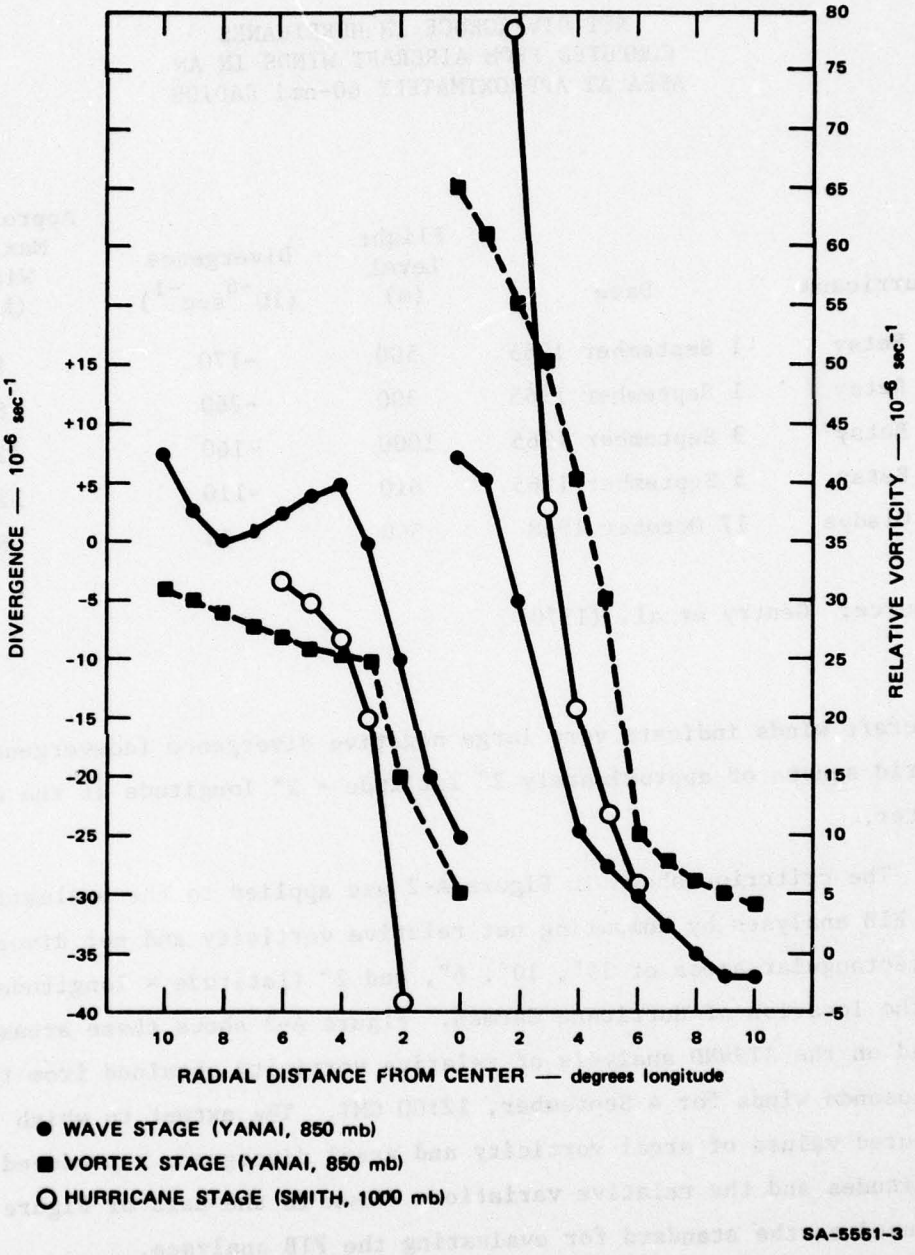

FIGURE A-2 EXAMPLES OF INCREASE IN RELATIVE CYCLONIC VORTICITY AND CONVERGENCE IN A DIRECTION TOWARD THE CENTER OF A TROPICAL STORM, AS COMPUTED FROM WIND OBSERVATIONS BY YANAI (1961) AND SMITH (1975)

Table A-1

NET DIVERGENCE IN HURRICANES
COMPUTED FROM AIRCRAFT WINDS IN AN
AREA AT APPROXIMATELY 60-nmi RADIUS

Hurricane	Date	Flight Level (m)	Divergence (10^{-6} sec^{-1})	Approximate Maximum Winds (kt)
Betsy	1 September 1965	500	-170	80
Betsy	1 September 1965	300	-260	80
Betsy	3 September 1965	1000	-160	125
Betsy	5 September 1965	610	-110	125
Gladys	17 October 1968	540	- 13	64

Source: Gentry et al. (1970)

aircraft winds indicate very large negative divergence (convergence) in a grid square of approximately 2° latitude × 2° longitude at the cyclone center.

The criterion shown in Figure A-2 was applied to the evaluation of the FIB analyses by computing net relative vorticity and net divergence in rectangular areas of 14°, 10°, 6°, and 2° (latitude × longitude) centered at the location of Hurricane Carmen. Figure A-3 shows these areas superposed on the ATSWND analysis of relative vorticity obtained from the radiosonde winds for 4 September, 12:00 GMT. The extent to which the computed values of areal vorticity and areal divergence reproduced the magnitudes and the relative variations shown in the data of Figure A-2 was used as the standard for evaluating the FIB analyses.

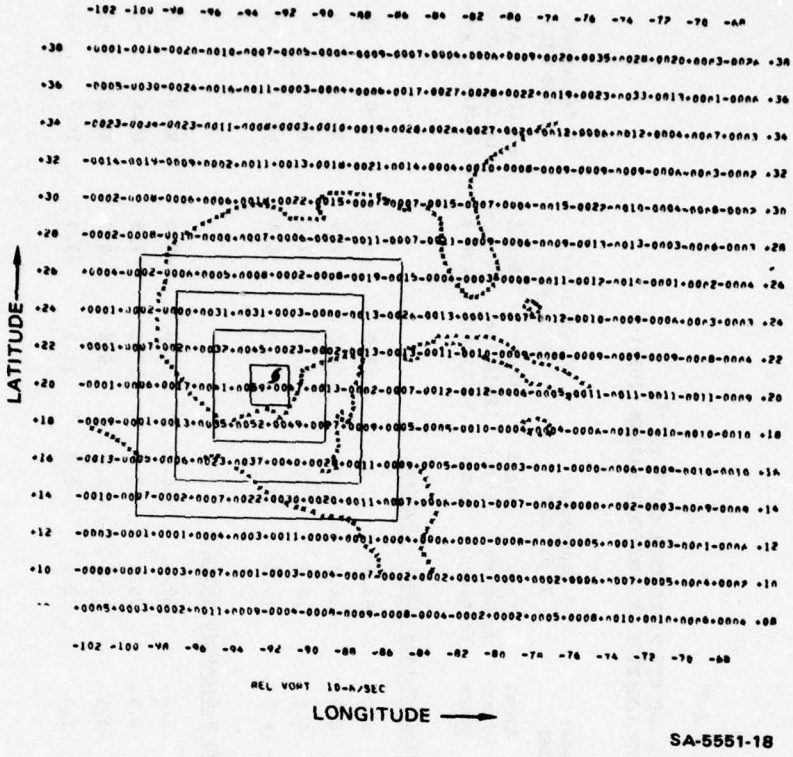

SA-5551-18

FIGURE A-3 AREAS OF 14°, 10°, 6°, AND 2° (LATITUDE X LONGITUDE) FOR WHICH NET RELATIVE VORTICITY AND DIVERGENCE WERE COMPUTED TO EVALUATE FIB ANALYSES FOR HURRICANE CARMEN

Areas superposed on ATSWND analysis of relative vorticity from RAWIN, 4 September 1974, 12:00 GMT.

3. Application of Evaluation Criterion to First Test Case Study

a. Examination of Initial ATSWND Analyses

As has been shown in Figure 1 Section III, ATSWND analyses of the CMV and RAWIN data provide the initial input to the FIB program. It therefore seems appropriate to first examine the quality of these analyses.

Table A-2 summarizes the results when the evaluation criteria outlined above are applied to the ATSWND-generated initial fields of relative vorticity and divergence obtained from the low-level cloud motion winds and the 850-mb radiosonde winds for 2 through 7 September. The listed

Table A-2

NET RELATIVE VORTICITY (10^{-6} SEC^{-1}) AND NET DIVERGENCE (10^{-6} SEC^{-1})
FOR VARIABLE GRID SQUARES CENTERED AT THE LOCATION OF HURRICANE CARMEN (1974)

Latitude × Longitude Grid Square (deg.)	2 September 12:00 GMT		3 September 12:00 GMT		4 September 12:00 GMT		5 September 12:00 GMT		6 September 12:00 GMT		8 September 00:00 GMT	
	Areal Relative Vorticity	Areal Diver-gence	Areal Relative Vorticity	Areal Diver-gence	Areal Relative Vorticity	Areal Diver-gence	Areal Relative Vorticity	Areal Diver-gence	Areal Relative Vorticity	Areal Diver-gence	Areal Relative Vorticity	Areal Diver-gence
From ATSWIND Low-Level Cloud Motion (Wind) Vectors												
2	40.0	4.0	69.0	-3.0	68.0	5.0	63.0	7.0	43.0	-5.0	52.0	19.0
6	18.1	1.6	35.5	1.2	41.6	6.0	34.3	2.8	34.5	2.5	34.3	4.0
10	5.9	2.2	17.7	2.4	20.9	7.5	17.7	2.6	15.9	7.0	19.1	-1.5
14	1.0	2.0	10.9	1.3	10.7	4.7	10.8	2.3	4.8	6.6	10.7	-0.6
From ATSWND 850-mb Radiosonde Winds												
2	23.0	-15.0	2.0	-2.0	47.0	1.0	30.0	-26.0	8.0	-8.0	93.0	6.0
6	18.3	-12.0	4.1	-4.8	34.8	-2.5	25.3	-13.6	17.5	-7.9	60.6	-3.8
10	10.7	-7.4	7.2	-3.8	24.2	-3.6	19.6	-10.7	16.8	-6.3	28.2	-1.6
14	4.9	-4.3	5.2	-0.9	14.1	-2.5	12.7	-8.2	11.1	-3.3	10.7	-1.4

GMT times correspond to the synoptic-chart times to which the satellite data are assumed to be applicable.

The increase in net relative cyclonic vorticity toward the hurricane center and the magnitude closest to the center computed from the low-level cloud motion (wind) vectors are in accordance with the vorticity criterion of Figure A-2 for each day of the period. Vorticity values computed from the 850-mb radiosonde winds show the correct trend, except for 3 and 6 September, for which some data at critical locations on the Yucatan Peninsula were missing. The cloud motion winds, however, are superior in representing relative vorticity. Figure A-4 shows the difference in data coverage between CMV and RAWIN for 3 September, when differences in net areal relative vorticity were large, according to Table A-2. The superior coverage of cloud motion winds around the cyclone center is obviously the reason for the good values of cyclonic vorticity computed from the cloud motion vector data.

The computations of net areal divergence shown in Table A-2 are inconsistent from day to day in terms of both trends and magnitudes. Only for 2 and 5 September, do the RAWIN data show good values. Divergence based on the CMV data, however, shows unrealistic trends and magnitudes.

Table A-2 suggests that divergence computed from CMV in the area of Hurricane Carmen is incompatible with the circulation of a tropical cyclone, while derived relative vorticity is meteorologically significant and should, therefore, be assigned high reliability (weight) in the FIB technique. Inaccurate height discrimination in the CMV data of the first test case may have been responsible for the unacceptable divergence values.

b. Examination of FIB Results

The FIB program was applied by blending vorticity and divergence computed from the cloud motion vector and radiosonde data.* Two different

*In subsequent discussions, relative vorticity and divergence computed from cloud motion vectors and radiosonde winds are designated as VORT (CMV), DIV (CMV) and VORT (RAWIN), DIV (RAWIN).

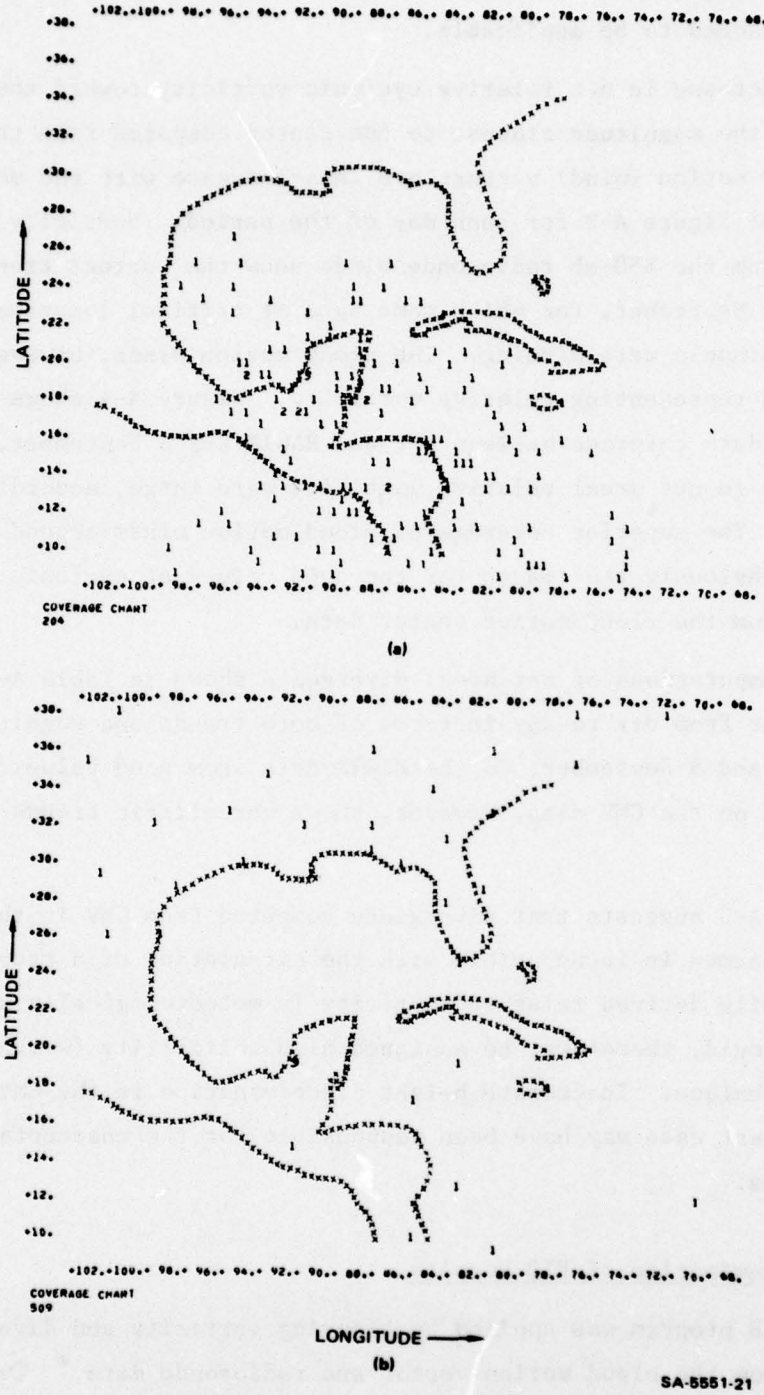

FIGURE A-4 DATA COVERAGE (1 OR 2 REPRESENTS NUMBER OF OBSERVATIONS) FOR 3 SEPTEMBER 1974, 12:00 GMT

(a) cloud motion winds
(b) radiosonde winds

cases with respect to the selection of new, independent data and background data were considered. In one case, the cloud motion winds were selected as the independent data and were blended with a background field based on radiosonde winds. In the other case, the radiosonde winds were assimilated in a background field based on the cloud motion data.

Values for the weighting factors A through D in Eq. (1), Section III, were chosen as A = 0.001 and B through D = 0.01. At the grid points where new, independent data were assembled, the weighting factor was set equal to 1.0. Thus, the gradient and curvature (Laplacian) properties of the background field were given much higher weight in the minimization solution of Eq. (1) than the scalar quantities, but the highest weight was assigned to the new data.

Results from the FIB program are summarized in Figure A-5 and are presented in the same graphical format as the data of Figure A-2, so that magnitudes and trends of vorticity and divergence can be evaluated by cross reference. The following features are noteworthy:

- The increase in relative cyclonic vorticity toward the hurricane center shows good positive correlation with that indicated by the vorticity data of Figure A-2 regardless of background choice. The anomaly in the analysis for 6 September using background (RAWIN) resulted from the ATSWND-computed background field of VORT(RAWIN), which included low values in the data-sparse area of the hurricane at grid points where no VORT(CMV) data were assembled. For all other days, any effects from the sparsity of rawinsonde data in the area of analysis were practically eliminated by the large number of assembled VORT(CMV) data weighted by 1.0. When the background was that associated with the cloud motion vectors, only a few assembled VORT(RAWIN) data were available, so the FIB results were again dominated by the CMV data. Thus, the CMV data always controlled the FIB analysis results, regardless of background choice, because of the dense CMV data coverage in an area of sparse radiosonde data.
- With the exception of 3 and 6 September (for the CMV background case), the FIB analyses of divergence reflect the unrealistic divergence values associated with the initial CMV data listed in Table A-2. Application of these values to the FIB program introduces meteorologically unacceptable effects into the solution of the blending equations.

To assess the effects of background gradients and curvature on the FIB analyses, the FIB program was applied to the data of the first test case, assuming B through D = 0. This assumption implies that the best

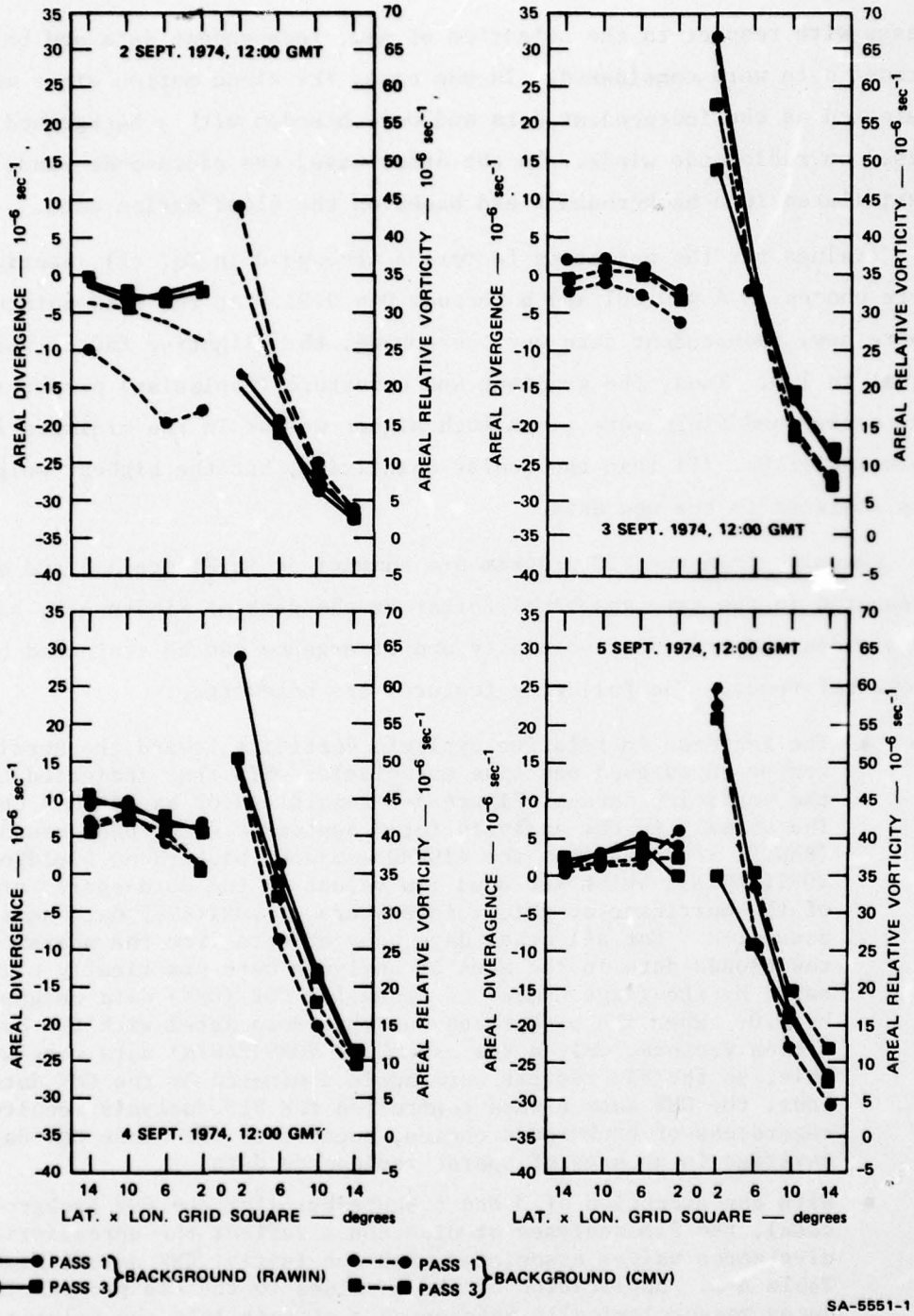

FIGURE A-5 FIB ANALYSIS RESULTS FOR THE FIRST TEST CASE, PRESENTED IN TERMS OF EVALUATION CRITERION OF FIGURE A-2

FIB Program was applied by utilizing vorticity and divergence computed from V(CMV) and V(RAWIN) with different background (first-guess) fields and DATAWT = 1.0, A = 0.001, B, C, D, E, F = 0.01.

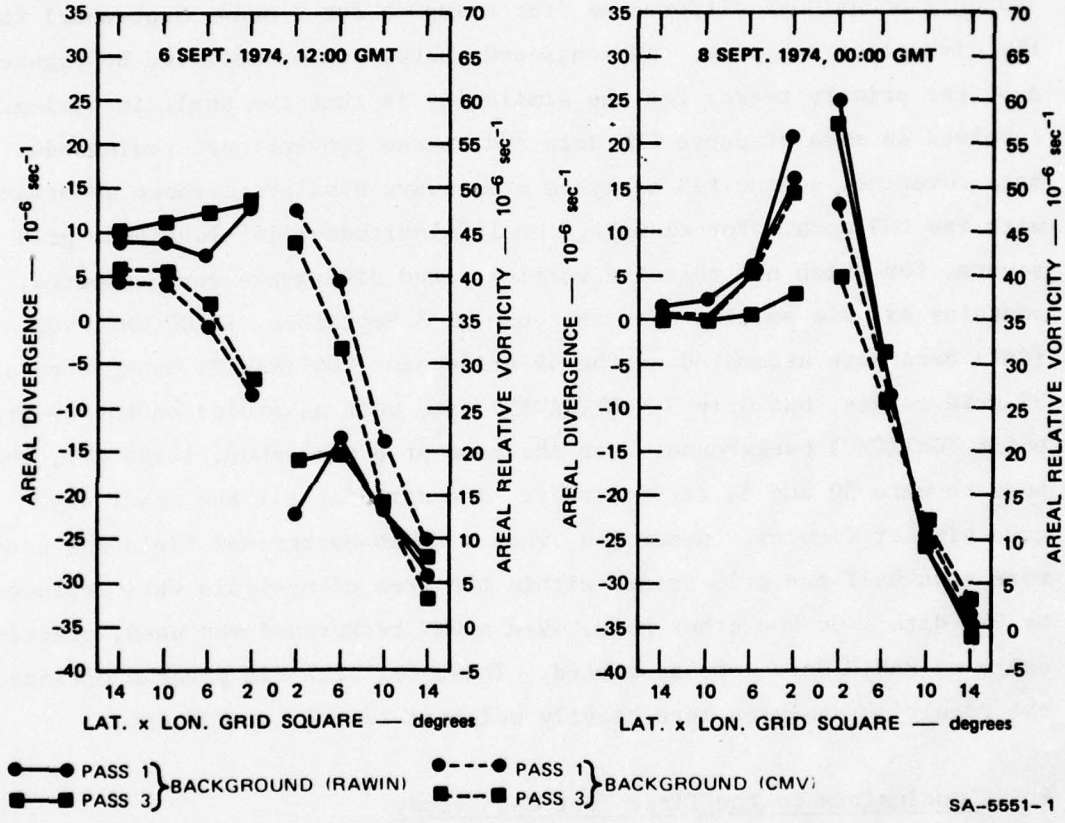

FIGURE A-5 (CONCLUDED)

available estimate of the true vorticity or divergence analysis equals the combined field of scalar background values and assembled data. No blending equation need be solved. The results for this specific case are summarized in Figure A-6.

Day-by-day comparison between the data of Figures A-5 and A-6 shows practically no difference in the FIB results for the vorticity analyses, and only occasional differences (for examples for 2 and 6 September) for the divergence analyses. As mentioned above, and exemplified by Figure A-5, the primary reason for the similarity is that the analysis evaluation involved an area of dense CMV data and sparse conventional radiosonde data coverage, so the FIB analyses are always similar to those associated with the CMV data. For example, the 14°-latitude-×-14°-longitude grid square, for which net relative vorticity and divergence were computed, contains 49 grid points. For the case of 3 September, 12:00 GMT, VORT (CMV) data were assembled on the 49-grid-point VORT(RAWIN) background at 39 grid points, but only 3 VORT(RAWIN) data were assembled on the 49-grid-point VORT(CMV) background. For the case of 5 September, 12:00 GMT, these numbers were 30 and 3, respectively. The data for all the other days gave similar figures. Generally, when a RAWIN background field was used, more than half the grid points within the area of analysis were replaced by CMV data. On the other hand, when a CMV background was used, practically no RAWIN data were assembled. Thus, for both FIB program options, the resulting analyses were heavily weighted toward the CMV data.

4. Conclusions to the First Test Case Study

From the preceding discussion, it is evident that divergence computed from the CMV data of the first test case study, and its subsequent assimilation through the FIB program, does not provide meteorologically acceptable analyses. Circulation, however, is an outstanding feature in the CMV data, especially in the synoptic situation associated with a tropical cyclone. Therefore, vorticity computed from the CMV data appears to be a meteorologically significant input into the FIB technique. This implies that only the rotational part of the cloud motion (wind) vectors contains useful information.

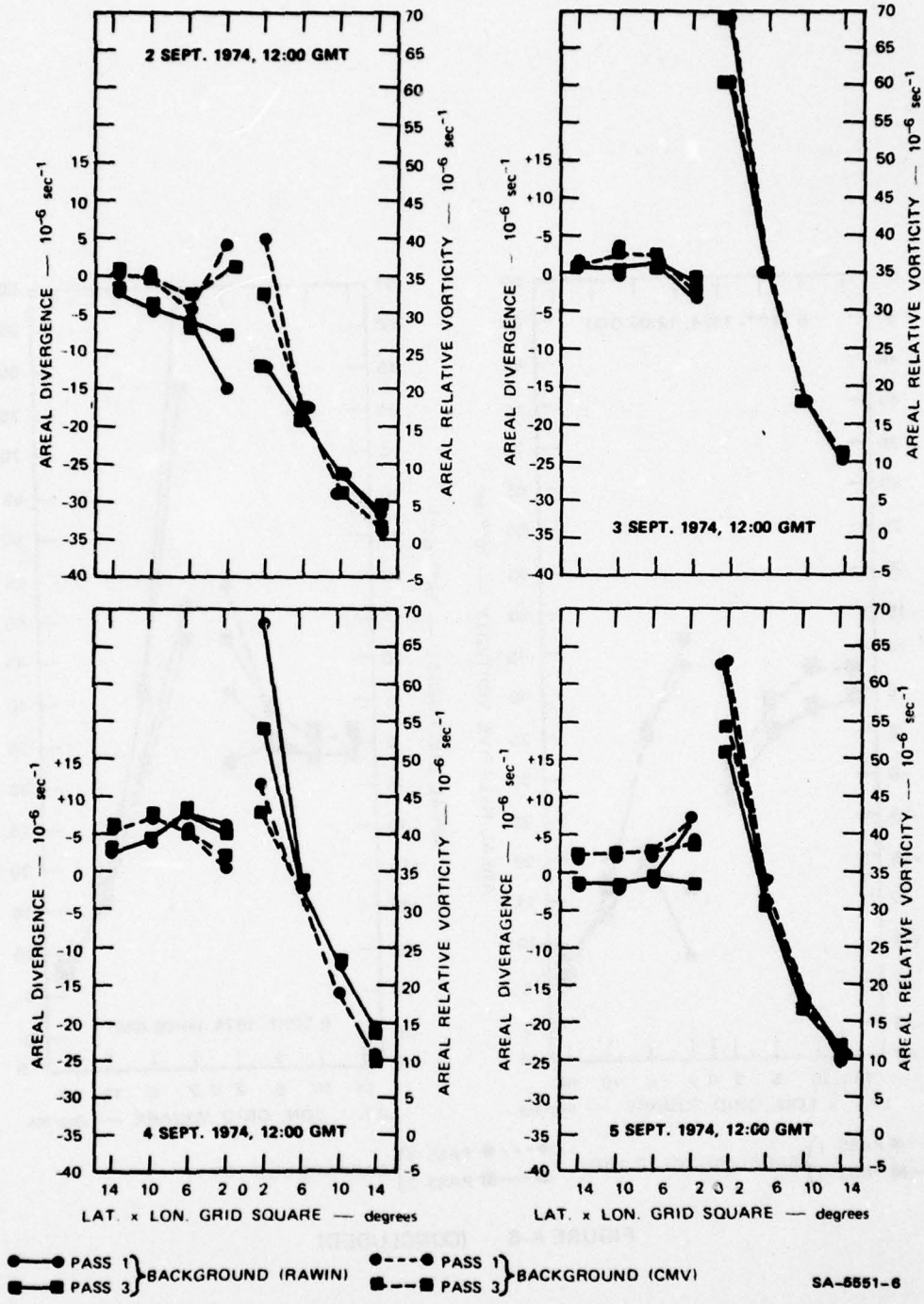

FIGURE A-6 FIB ANALYSIS RESULTS FOR THE FIRST TEST CASE, PRESENTED IN TERMS OF EVALUATION CRITERION OR FIGURE A-2

FIB program was applied by utilizing vorticity and divergence computed from V(CMV) and V(RAWIN) with different background (first-guess) fields and DATAWT = 1.0, A = 0.001, B, C, D, E, F = 0.

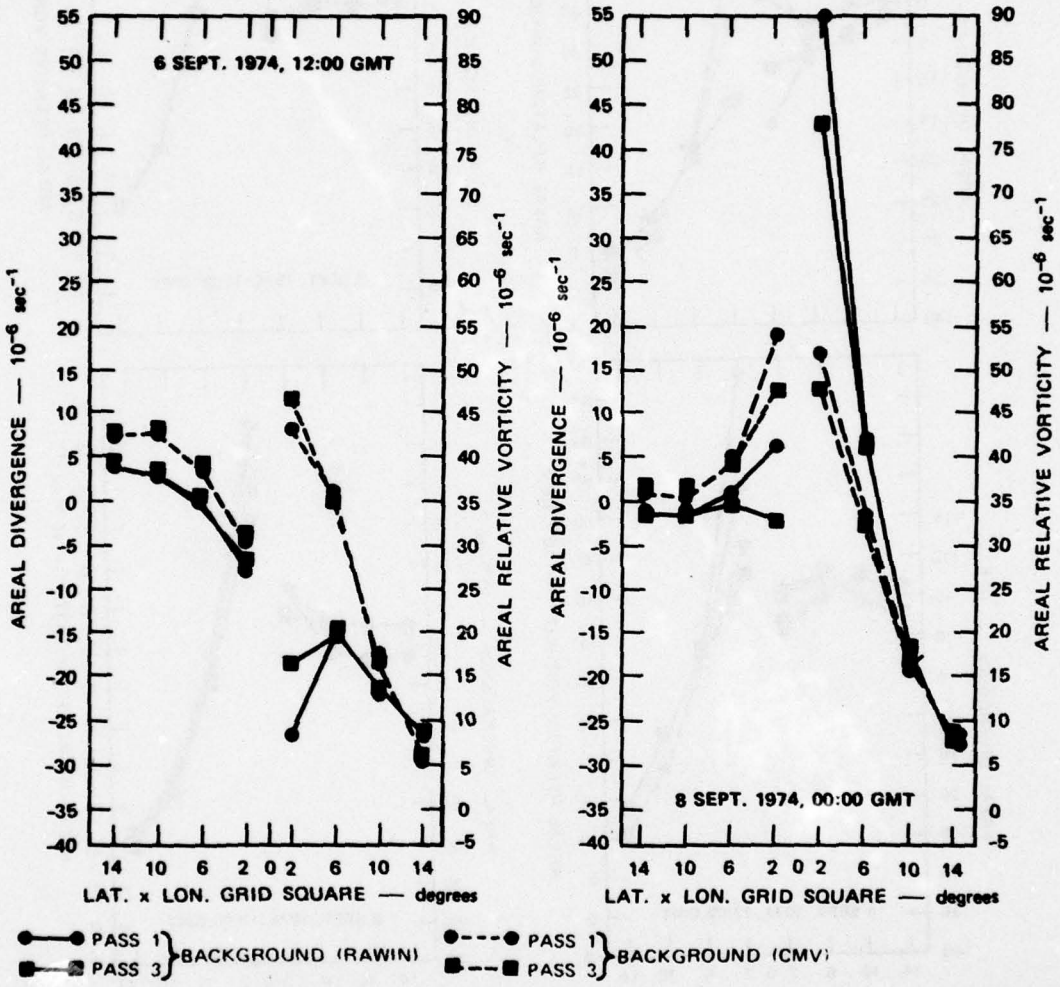

FIGURE A-6 (CONCLUDED)

Appendix B

SENSITIVITY OF FIB RESULTS TO BACKGROUND WEIGHTING FACTORS

Appendix B

SENSITIVITY OF FIB RESULTS TO BACKGROUND WEIGHTING FACTORS

1. Background Data

To explore the sensitivity of the FIB results for the first study case to changes in independent data weight and in background gradient weights (B through F), the low-level VORT(CMV) and the 850-mb VORT (RAWIN) data for 7 September 1974 were selected for further analysis. For this date, the ATSWND analysis of VORT(CMV) is based on dense coverage of low-level cloud motion vectors for the time period 18:47:00 through 21:10:00 GMT, while the corresponding VORT(RAWIN) analysis is based on the 850-mb rawinsonde data for 8 September, 00:00 GMT. The rawinsonde data analysis has high reliability because of the proximity of Hurricane Carmen to the relatively dense radiosonde network of the U.S. mainland.

Figure B-1 shows the coverage of low-level VORT(CMV) and 850-mb VORT (RAWIN). The corresponding patterns of VORT(CMV) and VORT(RAWIN) generated by ATSWND and analyzed in terms of isopleths of relative vorticity are shown in Figure B-2 within a 12°-latitude-×-12°-longitude area centered at Hurricane Carmen.

For the sensitivity study, the FIB technique was applied by using VORT(RAWIN) as the background field and VORT(CMV) as the independent data. The high reliability of the VORT(RAWIN) background is evident from its classical pattern of vorticity isopleths shown in Figure B-2(a) which satisfies the vorticity criterion for tropical cyclones: relative cyclonic vorticity sharply increases toward the hurricane center and reaches a maximum value of 92.6×10^{-6} sec^{-1}.

The encircled grid points on Figure B-2(a) are those at which VORT(CMV) data were assembled prior to solving the blending equation.

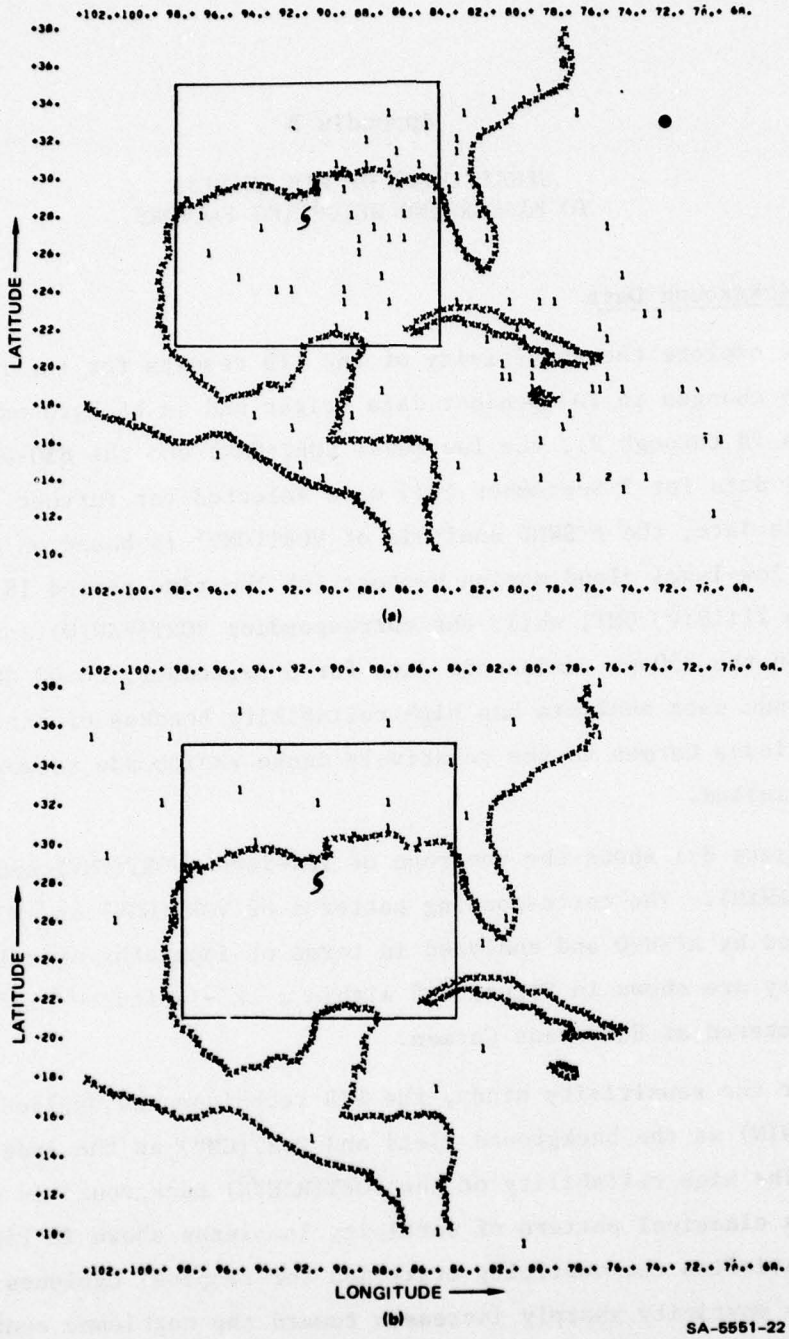

FIGURE B-1 COVERAGE CHART OF (a) LOW-LEVEL CLOUD MOTION VECTORS, 7 SEPTEMBER 1974, 18:47-21:10 GMT (b) 850-mb RAWINSONDE DATA, 8 SEPTEMBER 1974, 00:00 GMT
Boxes identify area of detailed VORT(FIB) analysis.

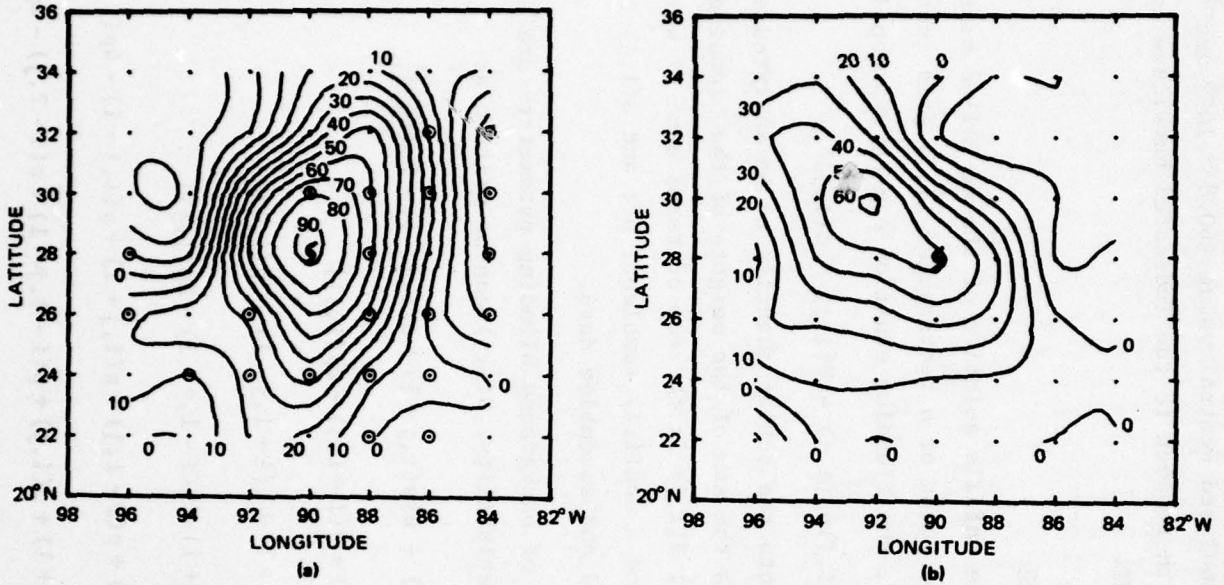

FIGURE B-2 ISOPLETHS OF RELATIVE VORTICITY (COMPUTER GENERATED FROM ATSWND) AT INTERVALS OF 10 X 10^{-6} sec^{-1} SHOWING VORTICITY PATTERNS ASSOCIATED WITH HURRICANE CARMEN AS ANALYZED FROM (a) BACKGROUND FIELD OF 850-mb VORT (RAWIN), 8 SEPTEMBER 1974, 00:00 GMT; (b) INDEPENDENT DATA FIELD OF LOW-LEVEL VORT (CMV), 7 SEPTEMBER 1974, 18:47-21:10 GMT

These grid points are closest to the locations of the CMV data [see Figure B-1(a)]. The vorticity pattern obtained from the cloud motion vectors shown in Figure B-2(b) is not as strong as that from the rawinsonde data, and the analyzed central value (60.8×10^{-6} sec^{-1} at 30°N, 92°W) is displaced with respect to the indicated hurricane location for 7 September, 18:00 GMT.

2. Blending Equation

The FIB technique entails solution of the so-called blending equation at every grid point of a rectangular (I,J) grid array. According to Maxwell (1976), the blending equation can be written in the form:*

$$S(i,j)p^*(i,j) - H(i,j) = G(i,j) \ , \qquad \text{(B-1)}$$

where $p^*(i,j)$ represents the scalar quantity to be analyzed at the grid point (i,j); S(i,j) is the sum of the weights of the blending parameters (DATAWT, A through F); H(i,j) is the sum of terms each of which is the product of a weight and a non(i,j) (ambient) p^*; and G(i,j) is a function only of the background and assembled data.

When the weights of background blending parameters are assigned without any spatial variability, G(i,j) can be written as

$$\begin{aligned} G(i,j) = {} & A(i,j)p'(i,j) - B[p(i,j+1) + p(i,j-1) - 2p(i,j)] \\ & - C[p(i+1,j) + p(i-1,j) - 2p(i,j)] \\ & - E[p(i-1,j+1) + p(i+1,j-1) - 2p(i,j)] \\ & - F[p(i+1,j+1) + p(i-1,j-1) - 2p(i,j)] \\ & -4D[p(i+1,j) + p(i-1,j) + p(i,j+1) + p(i,j-1) - 4p(i,j)] \\ & + D[p(i-1,j+1) + p(i,j) + p(i-1,j-1) + p(i-2,j) - 4p(i-1,j)] \\ & + D[p(i+1,j+1) + p(i,j) + p(i+1,j-1) + p(i+2,j) - 4p(i+1,j)] \end{aligned}$$

*Here, S(i,j) is equivalent to $S_{i,j}$.

$$+ D[p(i,j) + p(i+1,j-1) + p(i,j-2) + p(i-1,j-1) - 4p(i,j-1)]$$

$$+ D[p(i,j) + p(i+1,j+1) + p(i,j+2) + p(i-1,j+1) - 4p(i,j+1)]$$

In the above expressions, p represents the scalar quantity of the background field, and p' represents the independent information assembled at the grid point (i,j). If no independent datum is assembled, p' = p.

When the first gradients in the i and j directions and along the right and left diagonals are assigned equal weight (B = C ≡ W and E = F ≡ K), G(i,j) can be simplified as follows:

$$G(i,j) = A(i,j)p'(i,j) - W[p(i,j+1) + p(i+1,j) + p(i,j-1) + p(i-1,j) - 4p(i,j)]$$

$$- K[p(i-1,j+1) + p(i+1,j+1) + p(i+1,j-1) + p(i-1,j-1) - 4p(i,j)]$$

$$-4D[p(i,j+1) + p(i+1,j) + p(i,j-1) + p(i-1,j) - 4p(i,j)]$$

$$+ D[\text{Laplacian of p at } (i,j+1) + \text{Laplacian of p at } (i-1,j) +$$

$$\text{Laplacian of p at } (i,j-1) + \text{Laplacian of p at } (i+1,j)] .$$

Using the same assumptions, H(i,j) in Eq. (B-1) can be expressed similarly, and the blending equation can be written as

$$A(i,j)p^*(i,j) - W[p^*(i,j+1) + p^*(i+1,j) + p^*(i,j-1) + p^*(i-1,j) - 4p^*(i,j)]$$

$$- K[p^*(i-1,j+1) + p^*(i+1,j+1) + p^*(i+1,j-1) + p^*(i-1,j-1) - 4p^*(i,j)]$$

$$-4D[p^*(i+1,j) + p^*(i-1,j) + p^*(i,j+1) + p^*(i,j-1) - 4p^*(i,j)]$$

$$+ D[\text{Laplacian of } p^* \text{ at } (i,j+1) + \text{Laplacian of } p^* \text{ at } (i-1,j) +$$

$$\text{Laplacian of } p^* \text{ at } (i,j-1) + \text{Laplacian of } p^* \text{ at } (i+1,j)] =$$

$$A(i,j)p'(i,j) - W[p(i,j+1) + p(i+1,j) + p(i,j-1) + p(i-1,j) - 4p(i,j)]$$

$$- K[p(i-1,j+1) + p(i+1,j+1) + p(i+1,j-1) + p(i-1,j-1) - 4p(i,j)]$$

$$-4D[p(i,j+1) + p(i+1,j) + p(i,j-1) + p(i-1,j) - 4p(i,j)]$$

$$+ D[\text{Laplacian of } p \text{ at } (i,j+1) + \text{Laplacian of } p \text{ at } (i-1,j) +$$

$$\text{Laplacian of } p \text{ at } (i,j-1) + \text{Laplacian of } p \text{ at } (i+1,j)] \quad . \qquad \text{(B-2)}$$

Thus, under the assumption of no spatial variability in the background weights, and for B = C and E = F, the blending of VORT(CMV) data into the background field of VORT(RAWIN) consists only of blending parameters related to the Laplacian at (i,j) and the Laplacian at four surrounding grid points. Thus, the curvature of the vorticity isopleths at (i,j) and that at adjacent grid points are the blending parameters.

It is of interest to note that the assignment of a value to D in Eq. (B-2) adds an additional weight of 4D to W.

3. Application of Eq. (B-2) to FIB

The vorticity pattern associated with a tropical cyclone such as that shown in Figure B-2(a) is composed of concentric isopleths of relative cyclonic vorticity that sharply increase in magnitude toward the cyclone center. For such patterns, the gradients in the i and j direction should carry large weight ($B,C \gg 0$), and the cross gradients for the left and right diagonals need not be considered separately ($E = F = 0$). If there is no obvious reason to distinguish between B and C, $B = C \equiv W$, and Eq. (B-2) is applicable in the form

$$A(i,j)p^*(i,j) - W[p^*(i,j+1) + p^*(i+1,j) + p^*(i,j-1) + p^*(i-1,j) - 4p^*(i,j)]$$

$$+ D[\text{Laplacian of } p^* \text{ at } (i,j+1) + \text{Laplacian of } p^* \text{ at } (i-1,j) +$$

$$\text{Laplacian of } p^* \text{ at } (i,j-1) + \text{Laplacian of } p^* \text{ at } (i+1,j)] =$$

$$A(i,j)p'(i,j) - W[p(i,j+1) + p(i+1,j) + p(i,j-1) + p(i-1,j) - 4p(i,j)]$$

$$+ D[\text{Laplacian of } p \text{ at } (i,j+1) + \text{Laplacian of } p \text{ at } (i-1,j) +$$

$$\text{Laplacian of } p \text{ at } (i,j-1) + \text{Laplacian of } p \text{ at } (i+1,j)] \quad . \qquad \text{(B-3)}$$

The Laplacian term associated with the weighting factor 4D in Eq. (B-2) has been combined with the identical Laplacian term weighted by W.

First, we consider the sensitivity of the FIB results to W by setting D = 0 in Eq. (B-3). Consider the pattern of relative vorticity isopleths of VORT(RAWIN) background shown in Figure B-2(a). Because of its high reliability, we wish to conserve this background pattern in the application of the FIB technique. Therefore, a relatively large value should be assigned to W. The sensitivity of the FIB analysis after the first pass [VORT(FIB1)] for different values of W is illustrated in Figure B-3, using DATAWT = 1.0 and A = 0.001. The FIB results are presented in terms of isopleths of relative vorticity at intervals of 10×10^{-6} sec^{-1}.

For the special case W = 0 and D = 0, Eq. (B-3) reduces to

$$A(i,j)p^*(i,j) = A(i,j)p'(i,j) \ ,$$

and the vorticity analysis simply consists of the background VORT(RAWIN) with the assembled VORT(CMV) data superimposed. No blending is required. It is evident from Figure B-3 that, in this case, the relative vorticity isopleths represent a pattern that is incompatible with the highly reliable VORT(RAWIN) background field, because of pronounced double vorticity centers. When a weight is assigned to W, the secondary vorticity center is considerably reduced. The patterns of VORT(FIB1), however, do not significantly change from the pattern associated with W = 0.01 until W increases to 0.5 or 1.0. This implies that, using DATAWT = 1.0 and A = 0.001, the FIB analysis does not significantly reproduce the latitudinally elongated vorticity pattern of the background field until the weight of the Laplacian blending parameter is comparable to that of the assembled independent data.

Figure B-4 shows more explicitly the sensitivity of VORT(FIB1) to the changes in W. Each curve presents VORT(FIB1) as a function of W at a grid point where VORT(CMV) data were assembled. The ten grid-point locations in the VORT(RAWIN) background field can be identified by reference to Figure B-2(a). Significant changes in VORT(FIB1) require rather large values of W, unless the grid point is associated with relatively large curvature in the vorticity isopleths, as occurs, for example, at 24°N, 90°W and at 28°N, 96°W. In general, increasing

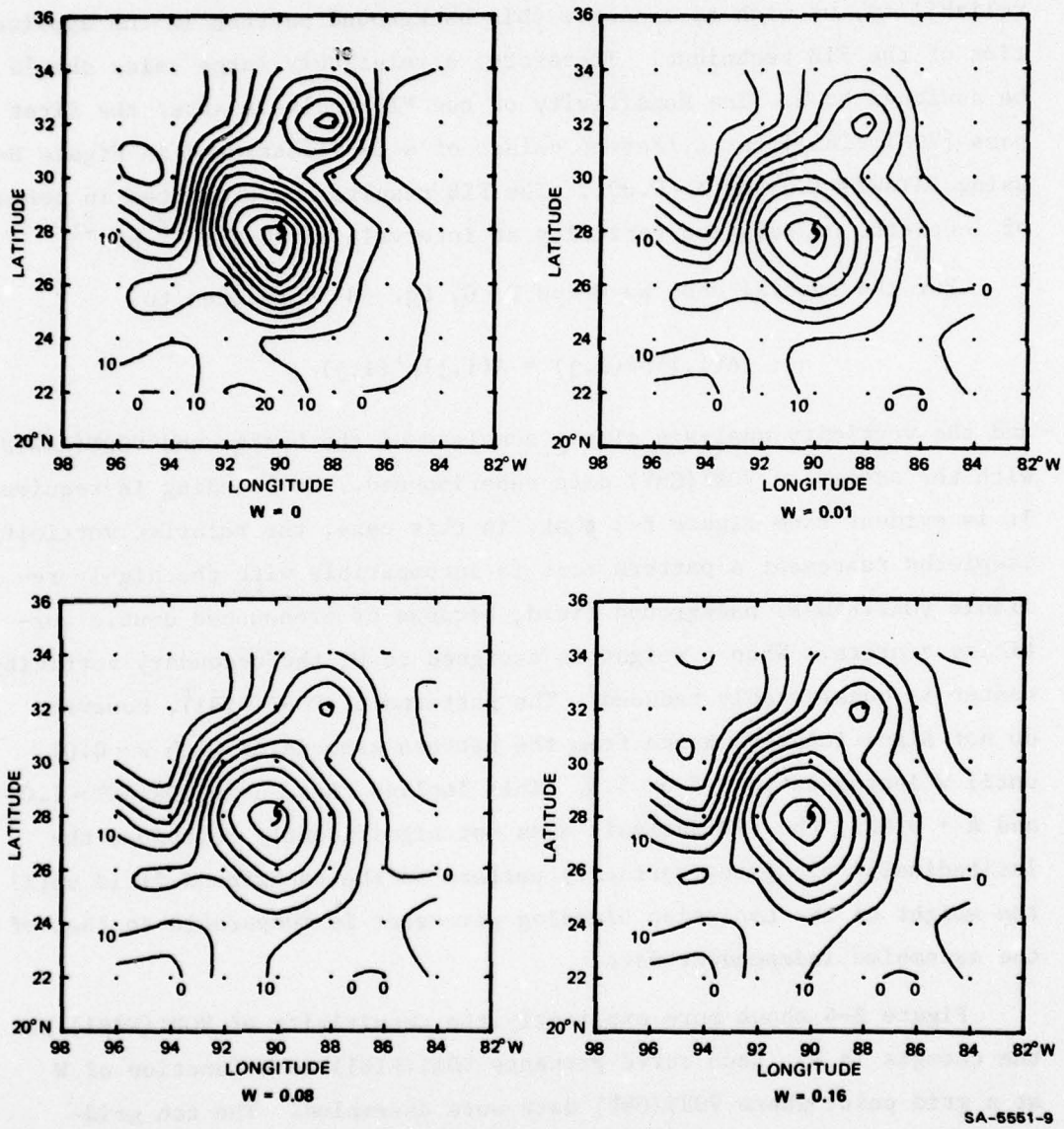

FIGURE B-3 ISOPLETHS OF RELATIVE VORTICITY AT INTERVALS OF 10×10^{-6} sec^{-1} OBTAINED FROM FIB TECHNIQUE USING DATAWT = 1.0, A = 0.001, D = 0, E = 0, F = 0, WITH DIFFERENT VALUES OF THE WEIGHTING FACTOR B = C = W.

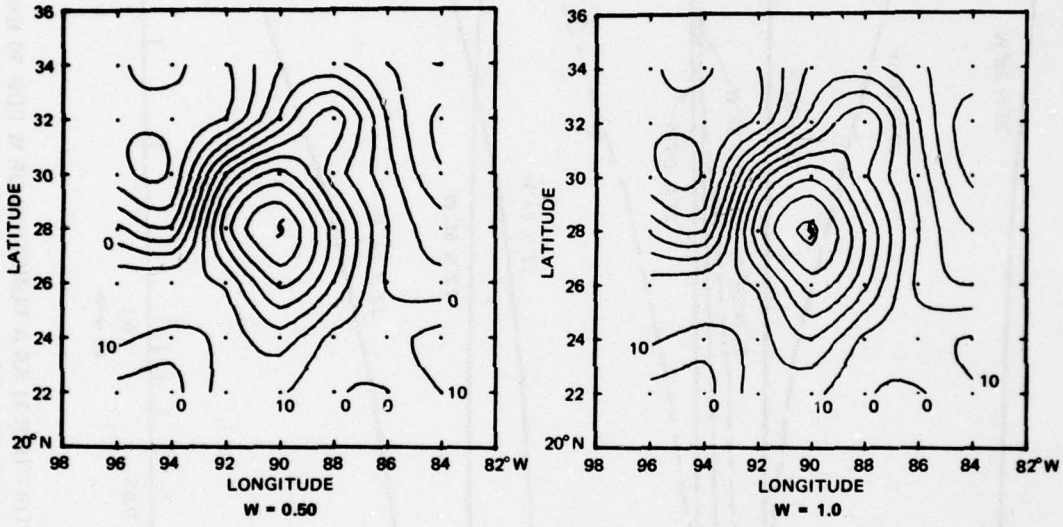

FIGURE B-3 (CONCLUDED)

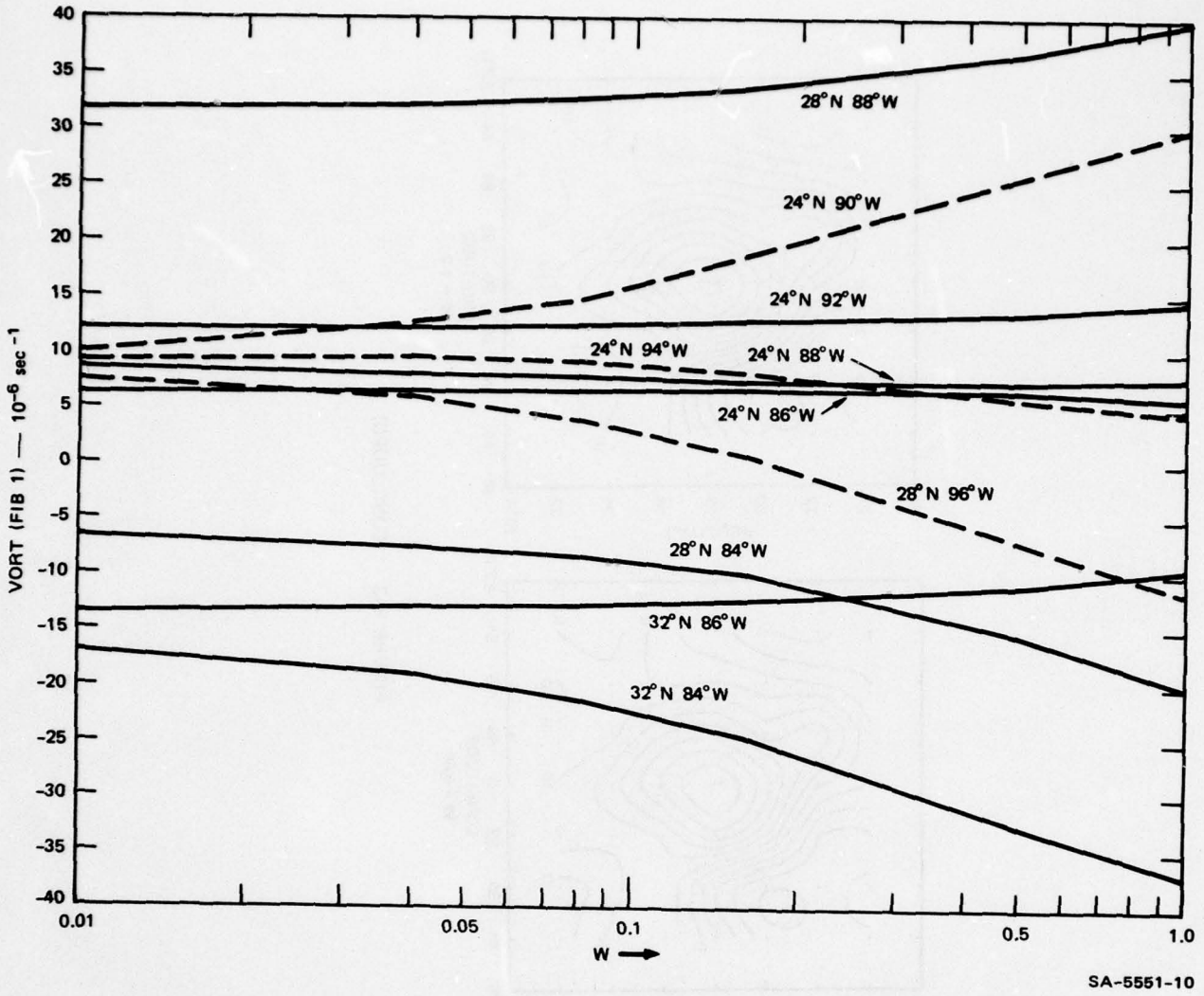

FIGURE B-4 VALUE OF VORT (FIB 1) AS A FUNCTION OF W FOR 10 GRID-POINTS [See Figure B-2 (a)] AT WHICH VORT (CMV) DATA WERE ASSEMBLED USING A = 0.001 AND DATAWT = 1.0

W = 0.01 by a factor of 10 to 20 does not result in significant changes in VORT(FIB1) because of the choice of DATAWT = 1.0 and the magnitude of the background Laplacian--that is, the value of G(i,j) [right-hand side of Eq. (B-3)] at any one grid point does not change significantly.

Small values of W would affect the VORT(FIB1) analysis much more than is shown in Figure B-4, if DATAWT were reduced proportionally which would be equivalent to dividing both sides of the blending equation (B-3) by the same factor. Thus, the value of W relative to that of DATAWT influences the FIB analysis. For example, the data of Figures B-3 and B-4 would not change if both DATAWT and W were divided by the same factor, provided DATAWT remained large relative to A = 0.001.

Figure B-5 shows G(i,j) as a function of W/DATAWT for the ten grid points of Figure B-4. As expected, the curves are similar to those of Figure B-4, and show that the solution to the blending equation, Eq. (B-3) does not significantly change until W/DATAWT > 0.2.

4. Preliminary Conclusions

When the FIB technique is applied to meteorological analyses that pertain to tropical cyclones, a simplified form of the blending equation may be used to assimilate vorticity computed from cloud motion vectors. The simplification is possible because of the pattern of near-concentric isopleths of cyclonic vorticity that is characteristic of a tropical cyclone and that reflects the large rotational component of the horizontal wind field.

The blending parameters in the simplified blending equation are related to only the Laplacian properties of the background (first-guess) field. The background forcing function G(i,j) can be expressed as:

$$G(i,j) \equiv A(i,j)p'(i,j) - W[\text{Laplacian of } p \text{ at } (i,j)] +$$
$$D[\text{Laplacian of } p \text{ at } (i,j+1) + \text{Laplacian of } p \text{ at } (i-1,j) +$$
$$\text{Laplacian of } p \text{ at } (i,j-1) + \text{Laplacian of } p \text{ at } (i+1,j)] .$$

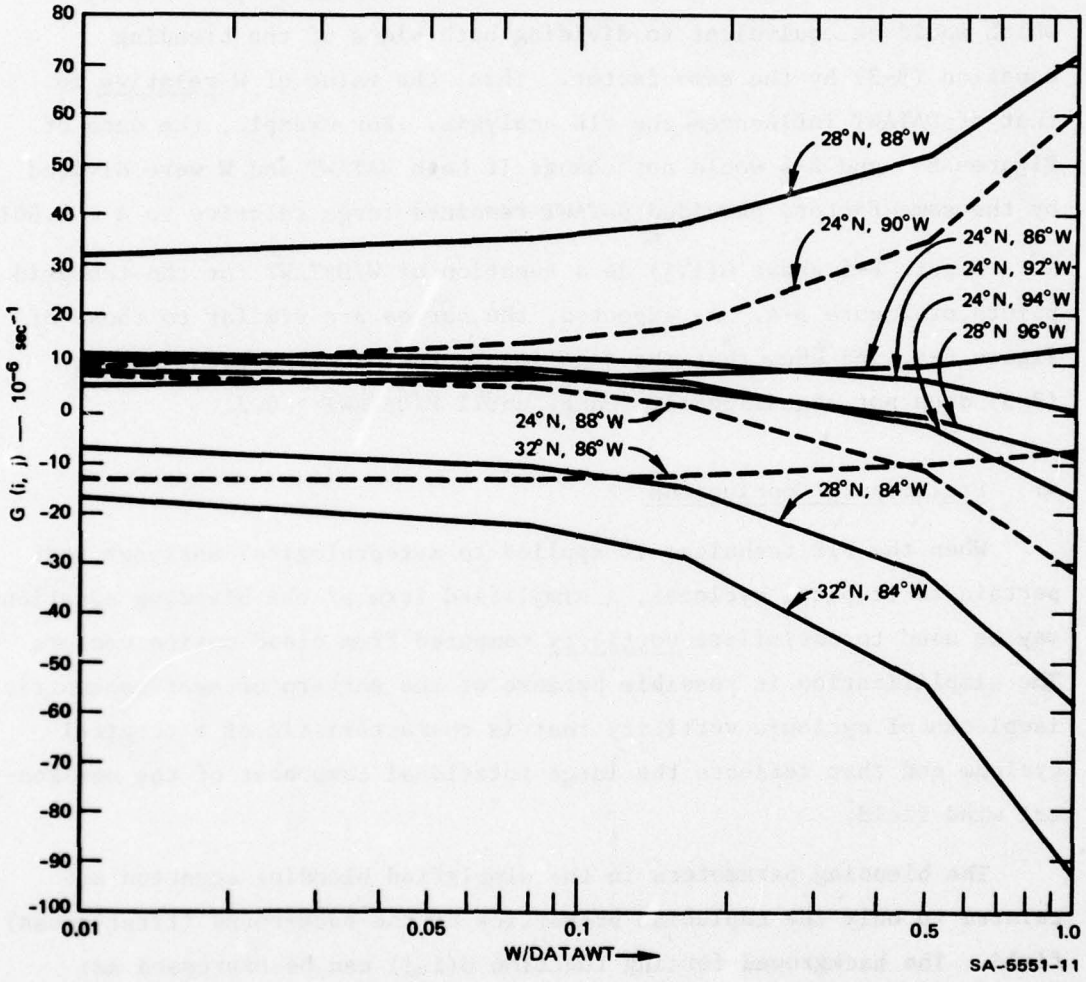

FIGURE B-5 FORCING FUNCTION G (i,j) AS A FUNCTION OF W/DATAWT FOR THE SAME 10 GRID-POINTS USED IN FIGURE B-4

In the sensitivity analysis discussed above, the influence on the FIB analysis of the Laplacian properties at the four grid points adjacent to (i,j) was omitted (D = 0). In this case, the background forcing function reduces to:

$$G(i,j) \equiv A(i,j)p'(i,j) - W[\text{Laplacian of } p \text{ at } (i,j)] \ , \qquad \text{(B-4)}$$

and the blending equation takes the form

$$A(i,j)p^*(i,j) - W[\text{Laplacian of } p^* \text{ at } (i,j)] = A(i,j)p'(i,j) - W[\text{Laplacian of } p \text{ at } (i,j)] \ . \qquad \text{(B-5)}$$

In our example of Figure B-3, A(i,j) = DATAWT + A = 1.001, and W = 0.01, 0.08, 0.16, 0.5, and 1.0. The above form of the blending equation shows that FIB results similar to those illustrated in Figure B-3 would have been obtained if DATAWT and W had been divided by, for example, a factor of 10. Thus, relative rather than absolute values of the weights control the FIB technique.

A proper choice of DATAWT and W can be made semiobjectively by (1) examining the initial fields of VORT(RAWIN) and VORT(CMV) generated by ATSWND, to determine the extent to which the background pattern should be conserved, and (2) computing the background Laplacian field and determining the values of W relative to DATAWT at which the forcing function [Eq. (B-4)] begins to change significantly. Two examples illustrate the approach.

Example A--7 September 1974

This example has been discussed in detail in preceding sections. Figure B-2 shows the ATSWND analyses of VORT(RAWIN) and VORT(CMV). The background field of VORT(RAWIN) has high reliability, and its pattern of relative vorticity should be conserved to a large extent. Figure B-5 shows that W should be > (0.2 DATAWT) to significantly change G(i,j) and, consequently, the solution to the blending equation.

Example B--6 September 1974

Figure B-6 shows the initial ATSWND analyses of VORT(RAWIN) and VORT(CMV) for 6 September 1974. The background field of VORT(RAWIN), which is valid for 12:00 GMT, is not representative of the vorticity pattern associated with a hurricane, because the area of analysis lies outside the network of available radiosondes. The superiority of the vorticity analysis obtained from the cloud motion vectors is evident from Figure B-6(b).

Obviously, no features in the background analysis of VORT(RAWIN) need to be conserved, and, therefore, the blending technique must be applied with minimum background weights. Figure B-7 shows the results of the FIB technique after the third blending loop and the 5-point smoothing. The blending equation is solved in the form given by Eq. (B-5), using DATAWT = 1.0, A = 0.001, B = C $\equiv$ W = 0.01. The pattern of relative vorticity obtained from the FIB technique [VORT(FIB3)] shows improvement over that of the VORT(RAWIN) background [Figure 6(a)]. The improvement, however, does not reflect the relatively large values ($>70 \times 10^{-6}$ sec^{-1}) associated with VORT(CMV) [See Figure B-6(b)]. One reason is that, prior to blending, values of VORT(CMV) are assembled only at the grid points closest to the location of the cloud motion vector data. Consequently, the large values in the VORT(CMV) analyses were not assembled [see Figure B-6(a)]. The FIB technique can be improved by modifying the program so that all values of the VORT(CMV) analysis are assembled, not only those closest to the location of the original cloud motion vectors.

An improved VORT(FIB) analysis could be obtained by using VORT(CMV) as the background (first-guess) field. The concept of assimilating available rawinsonde data into a background field of VORT(CMV), however, may not be desirable from an operational viewpoint. For example, conventional weather analyses obtained by numerical techniques are routinely provided, while CMV data can be expected to become available periodically in areas of extensive cloud cover. Therefore, it seems logical to periodically assimilate the CMV analyses into the conventional background analyses.

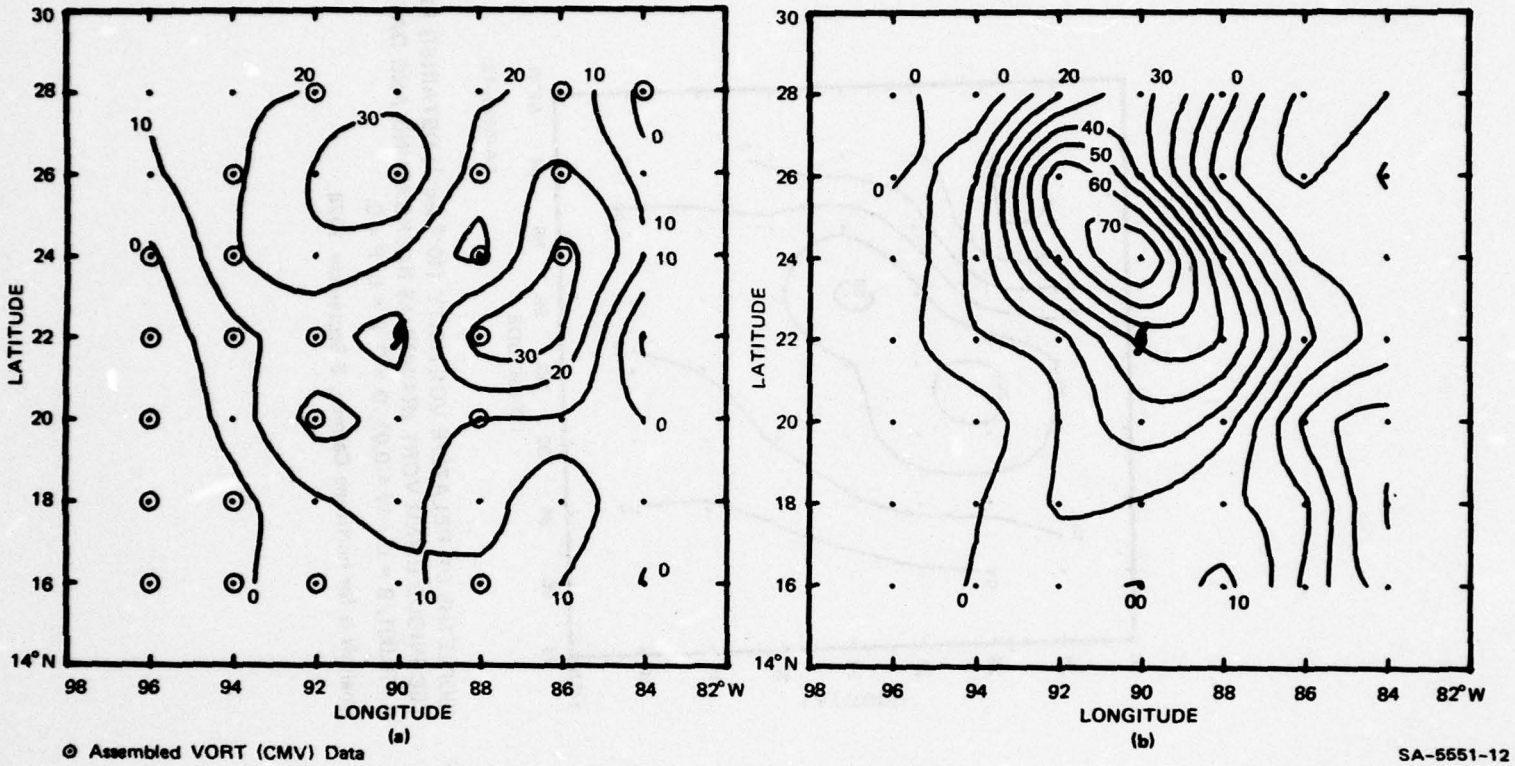

FIGURE B-6 PATTERNS OF RELATIVE VORTICITY (10^{-6} sec^{-1}) ASSOCIATED WITH HURRICANE CARMEN ON 6 SEPTEMBER 1974 AS OBTAINED BY ATSWND FROM (a) 850-mb RAWINSONDE DATA, 12:00 GMT; (b) LOW-LEVEL CLOUD MOTION VECTORS, 14:44-17:00 GMT

Indicated location of Hurricane Carmen valid for 12:00 GMT.

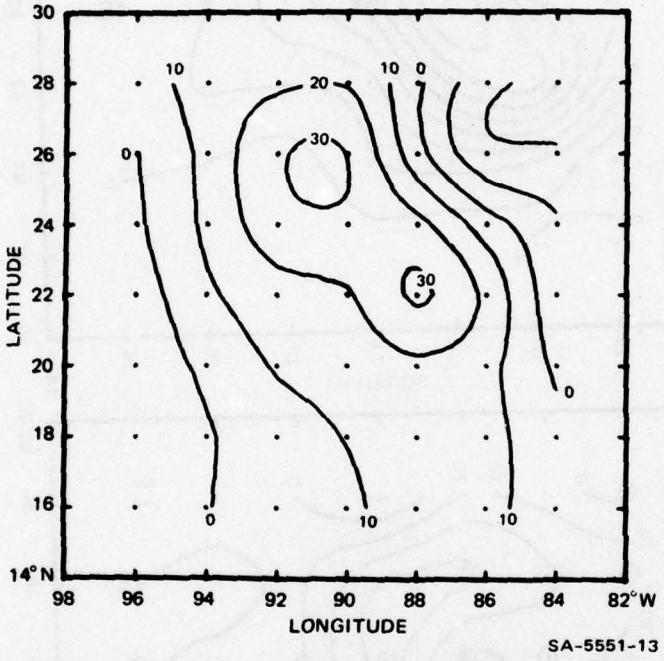

FIGURE B-7 ISOPLETHS OF RELATIVE VORTICITY (10^{-6} sec^{-1}) OBTAINED FROM FIB TECHNIQUE USING VORT (RAWIN) AS BACKGROUND AND DATAWT = 1.0, A = 0.001, B = C = W = 0.01, D = 0, E = 0, F = 0.

Analysis is for hurricane Carmen, 6 September 1974.

Appendix C

SECOND TEST CASE ANALYSES

Appendix C

SECOND TEST CASE ANALYSES

1. General

A second case study to evaluate the FIB technique for blending cloud motion data with conventional wind observations was carried out in the eastern Pacific Ocean from 20°N to 50°N and 120°W to 160°W. This case study involved the migration of an extratropical cyclone during the period 5 through 7 February 1976. Earth-located cloud motion vector (CMV) data were available as part of a NASA/NOAA-sponsored Data Systems Test (DST-6). Such tests are conducted as a prototype for the First GARP Global Experiment (FGGE). SMS-2 CMV data tapes were obtained from the Space Science and Engineering Center of the University of Wisconsin. Cloud motion (wind) vectors were generated on the University of Wisconsin McIDAS. CMV heights to the nearest 100 mb were determined from both the visible and infrared data.

The time periods for which CMV data were obtained are listed below. All data were for the 100-to-900-mb range and had full DISC coverage.

Date (Feb. 1976)	Time Period (GMT)
4	09:15-10:15
5	08:45-09:45 22:45-23:45
6	09:15-10:15 14:45-15:15 22:15-22:45
7	09:15-10:15 14:45-15:15
8	09:15-10:45

The background fields with which the independent CMV data were to be blended were the Fleet Numerical Weather Central (FNWC) constant-pressure height analyses for the levels and times closest to the heights and times of the CMV data. The background fields were generated from data tapes provided by the Technical Monitor.* The tapes contained contour height values for each of the 3969 points in the FNWC 63 × 63 operational grid for the standard constant-pressure levels and at the standard (GMT) times corresponding to the CMV data. A computer routine was developed to convert a given field of height values to a latitude/longitude field of geostrophic winds for the area of interest. The geostrophic winds as a function of latitude and longitude then provided the input to ATSWIND, which subsequently analyzed the background fields of wind, vorticity, and divergence on a 2°-latitude-×-2°-longitude grid mesh.

In view of the good representation of the rotational wind field by the cloud motion data of the first case study, and the simplification of the blending equation described in Appendix B, the second study was an evaluation of the FIB technique by blending CMV winds and geostrophic winds, using the respective vorticity properties and the solution to the simplified form of the blending equation. Divergence obtained from the CMV data was evaluated, but assimilation of this kinematic quantity in a background field based on geostrophic winds was not attempted, because of the nonrepresentativeness of the geostrophic divergence. The blending equation was applied to the second case study in its simplified form (see Appendix B) and solved by using the weighting factors listed in Table C-1.

Data blending using both low- and high-level winds was carried out for 6 and 7 February 1976, 00:00 and 12:00 GMT, and for 8 February, 00:00 GMT. The FIB technique and the blending procedure showed similar features for these five cases. One representative case (6 February, 00:00 GMT) has been described in Section IV. An additional case (7 February 1976,

---

*Mr. James Clark of NEPRF.

Table C-1

SUMMARY OF WEIGHTING FACTORS
USED IN FIB SOLUTION

Weighting Factor	Weight	Assigned Value
New data	DATAWT	1.0
Background scalar	A(i,j)	0.001
Gradient in j direction	B(i,j)	1.0
Gradient in i direction	C(i,j)	1.0
Cross gradients	E(i,j),F(i,j)	0
Laplacian	D(i,j)	0

00:00 GMT) is discussed in this Appendix. All other cases are summarized as to the significance of the blended end products.

2. Case Study of 7 February 1976, 00:00 GMT

(1) Application of FIB, using low-level winds.

(a) Initial Input Data Analyses

Figure C-1 shows the SMS-2 visible cloud images for 6 February 1976, 22:45 GMT, and the corresponding low-level (900- and 800-mb) CMV winds for 22:15-22:45 GMT. Figure C-2 shows the ATSWND analyses of the CMV data and the FNWC 850-mb geostrophic winds valid for 7 February 1976, 00:00 GMT. The circulation in the geostrophic wind field associated with the extratropical cyclone off the California coast and the anticyclone further westward are clearly defined by the CMV winds. However, when relative vorticity is computed from the data of Figure C-2, the CMV winds show various small-scale anomalies, as illustrated in Figure C-3. While the FNWC geostrophic winds represent a smooth synoptic-scale cyclonic relative vorticity pattern consistent with that associated with the extratropical cyclone,

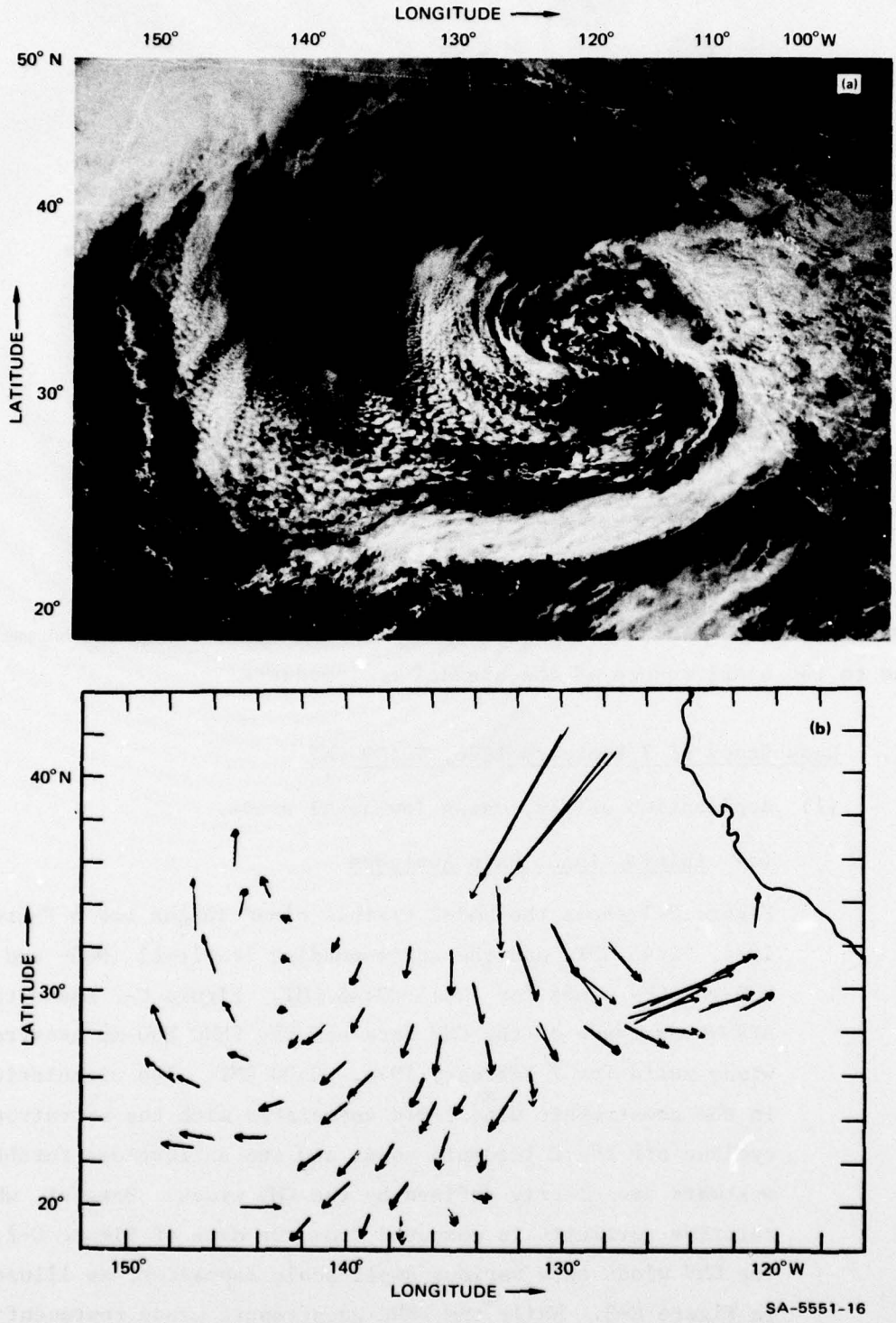

FIGURE C-1 SAMPLE OF SATELLITE DATA USED IN FIB TECHNIQUE

(a) SMS-2 visible cloud images, 6 February 1976, 22:45 GMT;

(b) Low-level cloud motion vectors, 6 February 1976, 22:15-22:45 GMT

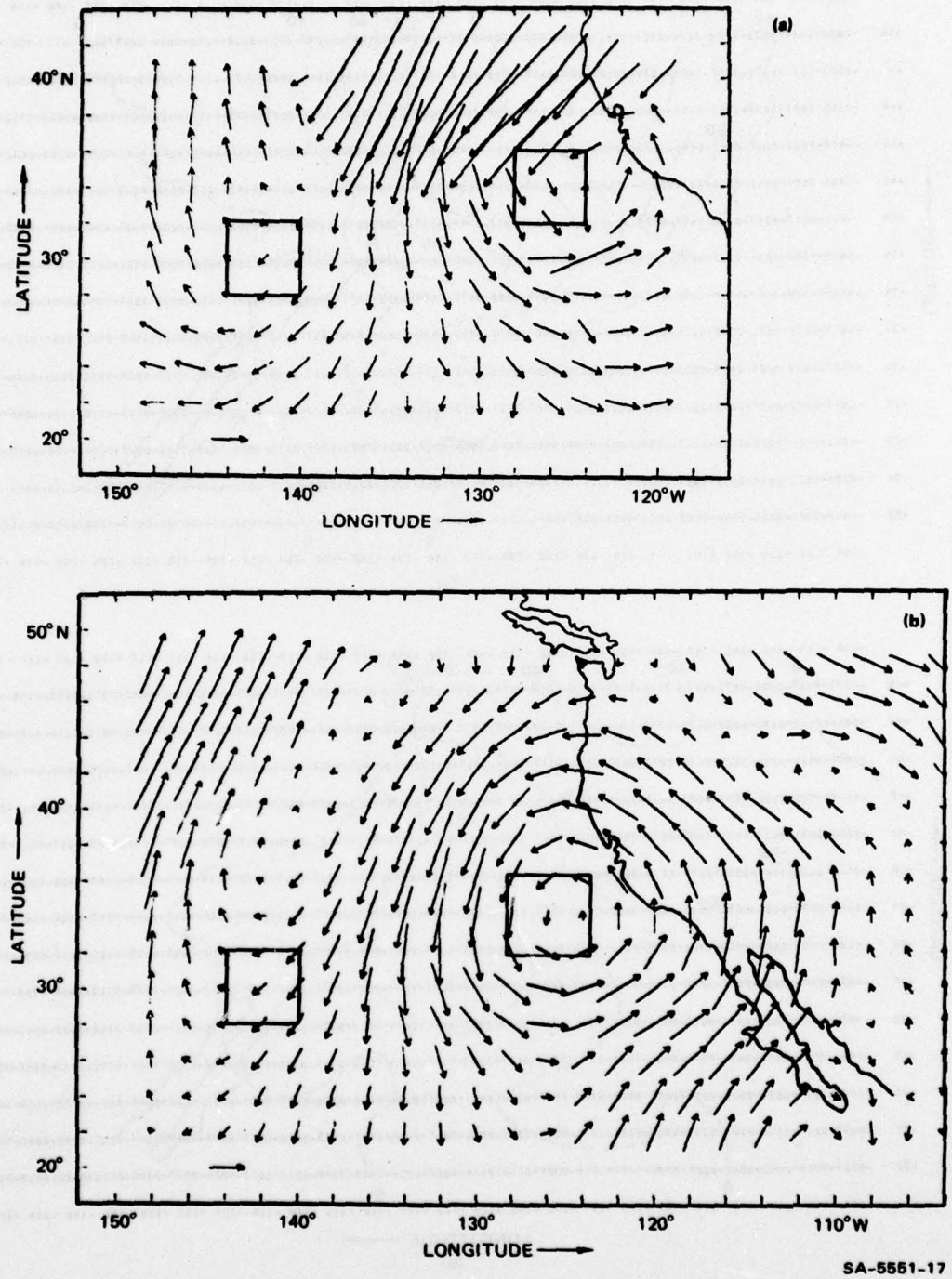

FIGURE C-2 SAMPLE OF LOW-LEVEL DATA ANALYSES USED IN FIB TECHNIQUE

(a) ATSWND analysis of CMV winds, 6 February 1976, 22:15-22:45 GMT

(b) ATSWND analysis of FNWC 850-mb geostrophic winds, 7 February 1976, 00:00 GMT

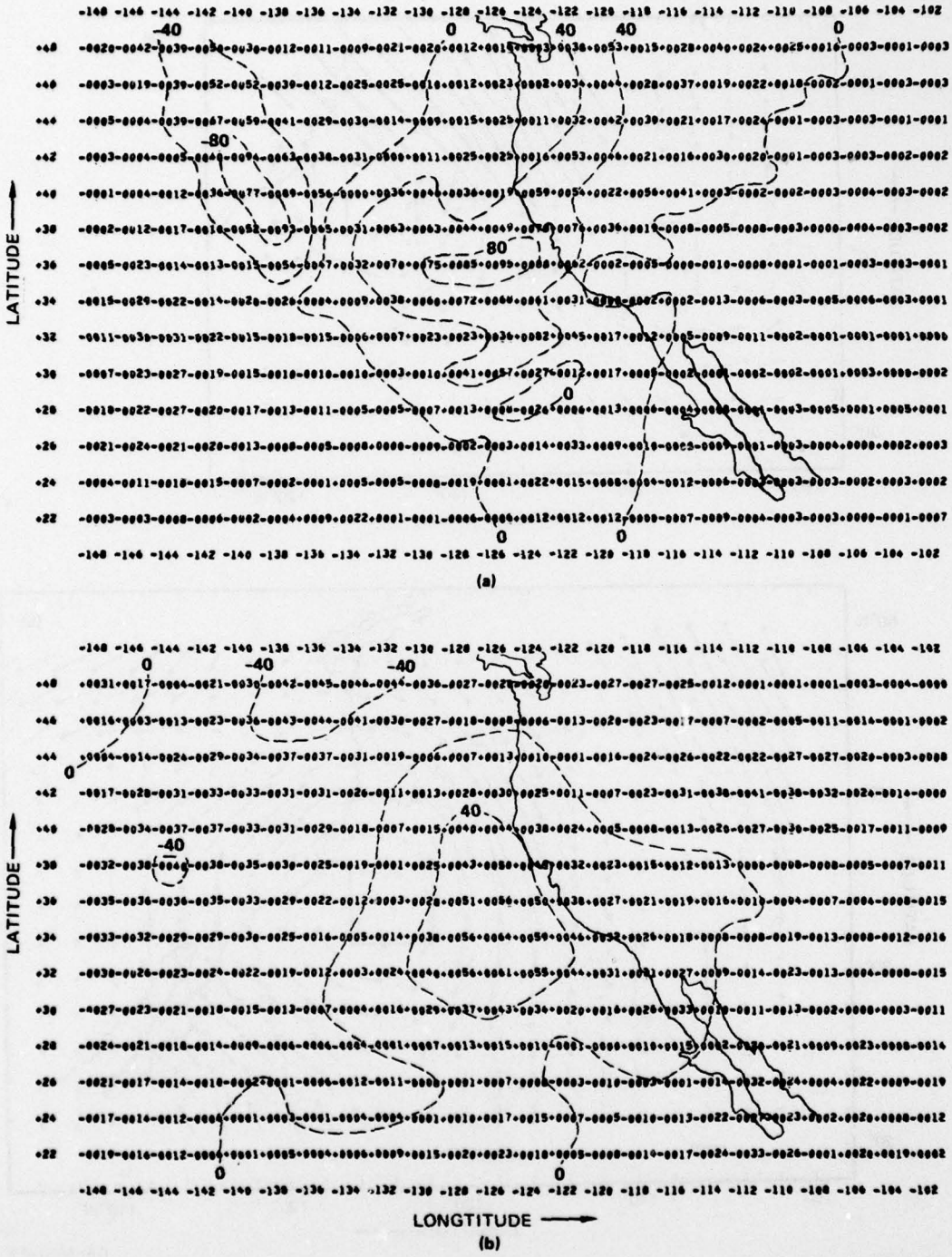

SA-5551-18

FIGURE C-3 ATSWND ANALYSIS OF RELATIVE VORTICITY (10^{-6} sec^{-1}) USED IN FIB TECHNIQUE AND OBTAINED FROM (a) LOW-LEVEL CMV WINDS, 6 FEBRUARY 1976, 22:15-22:45 GMT; (b) FNWC 850-mb GEOSTROPHIC WINDS, 7 FEBRUARY 1976, 00:00 GMT

the CMV winds produce small areas of anticyclonic vorticity east of the cyclone center. Whether these areas reflect mesoscale features or inaccuracies in the CMV data cannot be determined. During operational application of such data, however, a decision must be made whether to maintain such anomalies or edit them out of the CMV data. Since this research study was concerned with a test and evaluation of FIB, the anomalies were kept in the initial CMV input data so as to assess their effect on the objective FIB analysis.

(b) Independent Data Assembly

To initiate the blending cycle, a set of new independent VORT (CMV) data must be assembled in the VORT(V_g) background field. The independent data set is obtained by selecting the grid-point values in the ATSWIND analysis of VORT(CMV) [Figure C-3 (a)] that are nearest to the actual location of the cloud motion winds of Figure C-1(b). These values are subsequently assembled at the corresponding grid points in the ATSWIND background analysis of VORT(V_g) in Figure C-3(b).

(c) Evaluation of FIB Results

The impact of the VORT(CMV) data of Figure C-3(a) on the background field of geostrophic vorticity of Figure C-3(b) after application of the data blending technique is illustrated in Figure C-4. This figure shows grid-point values of the difference between the original background field of geostrophic vorticity [VORT(V_g)] and the FIB analysis of blended vorticity [VORT(FIB)] before and after so-called weight reevaluation. In Figure C-4(a), before weight reevaluation, geostrophic cyclonic vorticity east and south of the extratopical cyclone center has been reduced by the assimilation of the CMV data. This impact is apparent from the initial input data of Figure C-3: the small areas with anticyclonic vorticity in the CMV data are responsible for the reduction. When this reduction

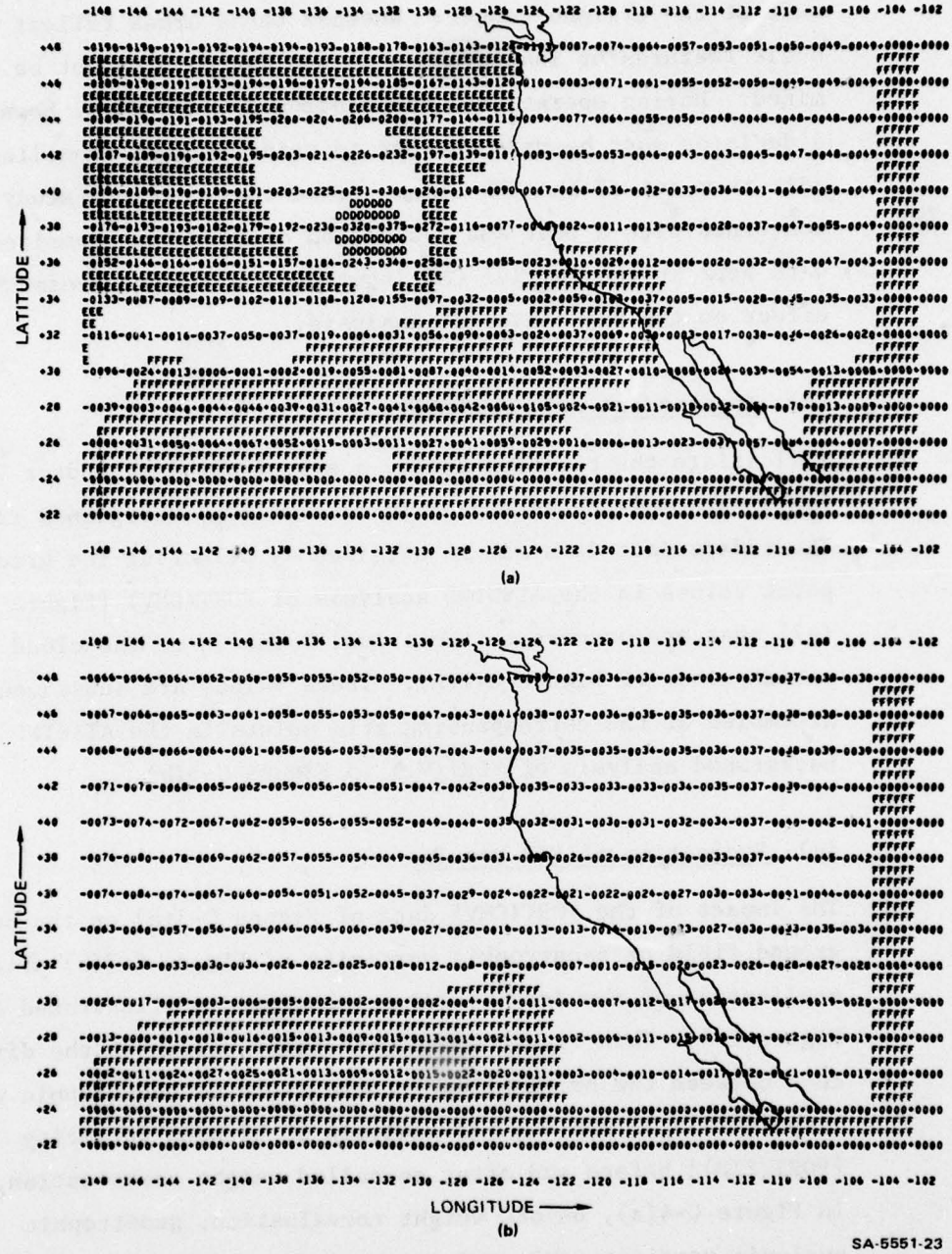

FIGURE C-4 RELATIVE VORTICITY DIFFERENCE (10^{-7}sec^{-1}) BETWEEN ORIGINAL BACKGROUND FIELD AND FIB ANALYSIS [VORT (Vg)-VORT (FIB)] FOR LOW-LEVEL WINDS
(a) BEFORE WEIGHT REEVALUATION; (b) AFTER WEIGHT REEVALUATION

Machine contouring denotes: D = <-30.0 x 10^{-6} sec^{-1}; E = -10.0 to -20.0 x 10^{-6} sec^{-6}; F = 0 to + 10.0 x 10^{-6} sec^{-1}.

in cyclonic relative vorticity is not accepted, the weight reevaluation routine is applied to the data of Figure C-4(a). For a detailed discussion of the weight reevaluation routine, see Maxwell (1976). In our study, the average standard deviation of the FIB solution from the background was limited to about 1.0. Whenever it exceeded 1.0, a new data weight was assigned and an improved solution to the blending equation was obtained. The overall improved FIB analysis is shown in Figure C-4(b). Increased conformity to the background is evident.

(2) Application of FIB, Using High-Level Winds

(a) Initial Input Data Analyses

Figure C-5 shows a high-level (300-mb) data sample used to evaluate the FIB technique. The SMS-2 cloud images corresponding to the CMV winds are those of Figure C-1(a). The ASTWND analysis of the 300-mb CMV winds [Figure C-5(b)] has discrepancies in the area of no data; otherwise, it represents the general circulation features of the FNWC 300-mb geostrophic wind field quite well. Differences between the cloud motion winds and the geostrophic winds are more evident in the analyses of relative vorticity shown in Figure C-6. In the area of cloud motion data coverage, many anomalies are present, and magnitudes of relative vorticity are much lower than those of geostrophic vorticity.

(c) Evaluation of FIB Results

The impact of the high-level cloud motion winds on the 300-mb geostrophic vorticity field is shown in Figure C-7 before and after weight reevaluation. Differences are shown between the original background of geostrophic vorticity and the results of the FIB analyses. Positive differences in the area of the extratopical cyclone indicate that [VORT(V_g)-VORT(FIB)] > 0, so cyclonic relative vorticity was reduced by the blending technique.

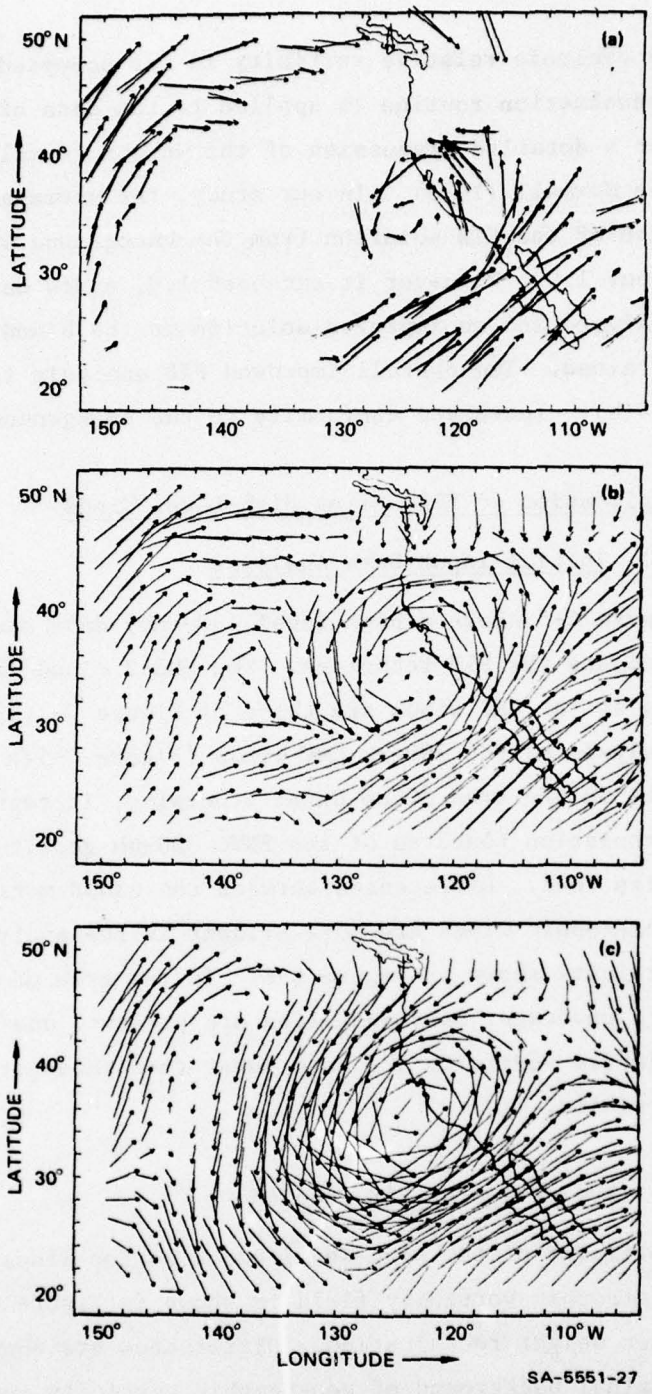

FIGURE C-5 SAMPLE OF HIGH-LEVEL ANALYSES USED IN FIB TECHNIQUE

(a) Coverage of high-level CMV winds, 6 February 1976, 22:15-22:45 GMT
(b) ATSWND analysis of high-level CMV winds
(c) ATSWND analysis of FNWC 300-mb geostrophic winds, 7 February 1976, 00:00 GMT

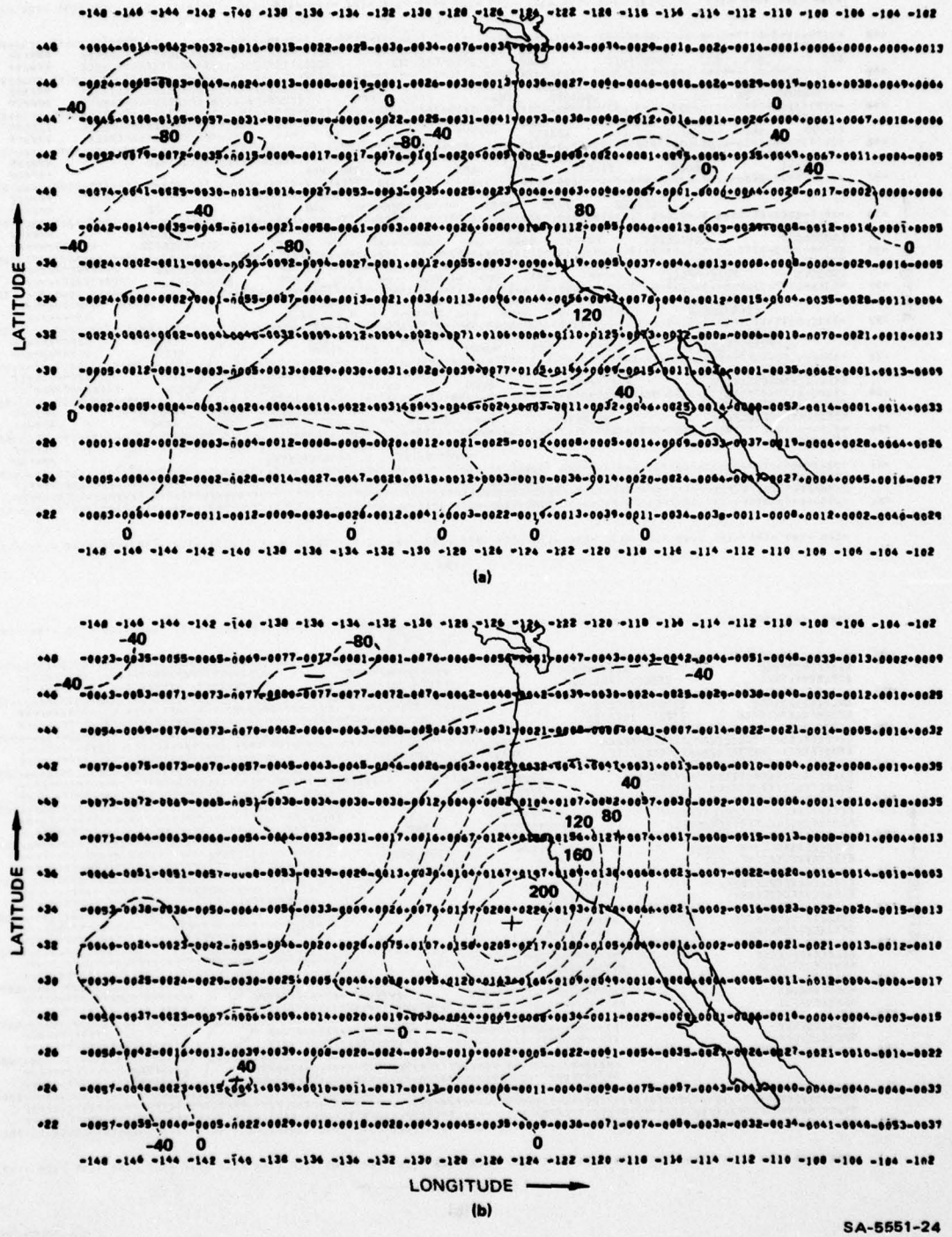

FIGURE C-6 ATSWND ANALYSIS OF RELATIVE VORTICITY (10^{-6}sec^{-1}) USED IN FIB TECHNIQUE AND OBTAINED FROM (a) HIGH-LEVEL CMV WINDS, 6 FEBRUARY 1976, 22:45-23:45 GMT; (b) FNWC 300-mb GEOSTROPHIC WINDS, 7 FEBRUARY 1976, 00:00 GMT

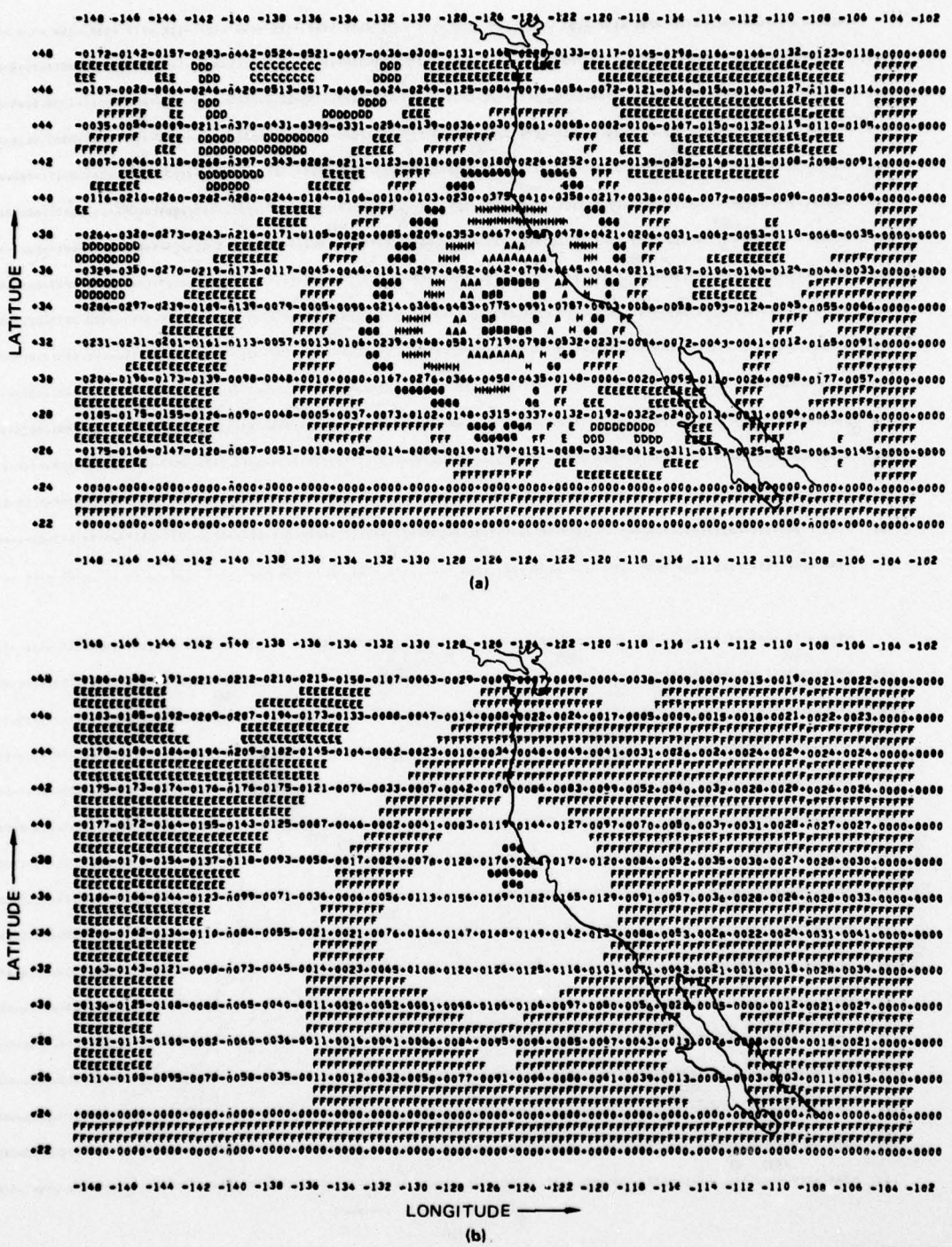

SA-5551-25

FIGURE C-7 RELATIVE VORTICITY DIFFERENCE (10^{-7} sec^{-1}) BETWEEN ORIGINAL BACKGROUND FIELD AND FIB ANALYSIS [VORT (Vg)-VORT (FIB)] FOR HIGH-LEVEL WINDS (a) BEFORE WEIGHT REEVALUATION; (b) AFTER WEIGHT REEVALUATION

3. Summary

The FIB results of the second test case study are summarized in Figure C-8. For four different times, average relative vorticity was computed over variable mesh-size grid squares centered at the extratropical cyclone (upper frames of Figure C-8) and at the anticyclone (lower frames). Grid squares of 18°, 14°, 10°, 6°, and 2° latitude × longitude were selected.

The vorticity computations, shown on the right-hand side of each frame were carried out using:

- The ATSWND analyses of relative vorticity obtained from the "independent" cloud motion winds and from the "background" FNWC geostrophic winds.
- The blended FIB analyses of relative vorticity before and after the weight reevaluation.

Average divergence was computed over the same grid squares only from the ATSWND analyses of divergence obtained from the "independent" cloud motion winds.

The vorticity data reflect the same features as the grid-point analyses presented in previous sections: In all cases, there is initially, a significant difference in magnitude of relative vorticity between the cloud motion winds and the geostrophic winds. The sign and the general trend of the vorticity, however, are similar. The cloud motion data correctly represent the extratropical cyclone as associated with large cyclonic vorticity increasing toward its center, and the anticyclone with negative relative vorticity. The impact of the cloud motion winds on the geostrophic background field is clearly demonstrated.

The average divergence associated with the cloud motion winds is more difficult to evaluate, since divergence pattern can be asymetric, depending on the movement and intensification of the extratopical cyclone. Analyses more detailed in time and space than carried out in this study are required to evaluate the blending of divergence.

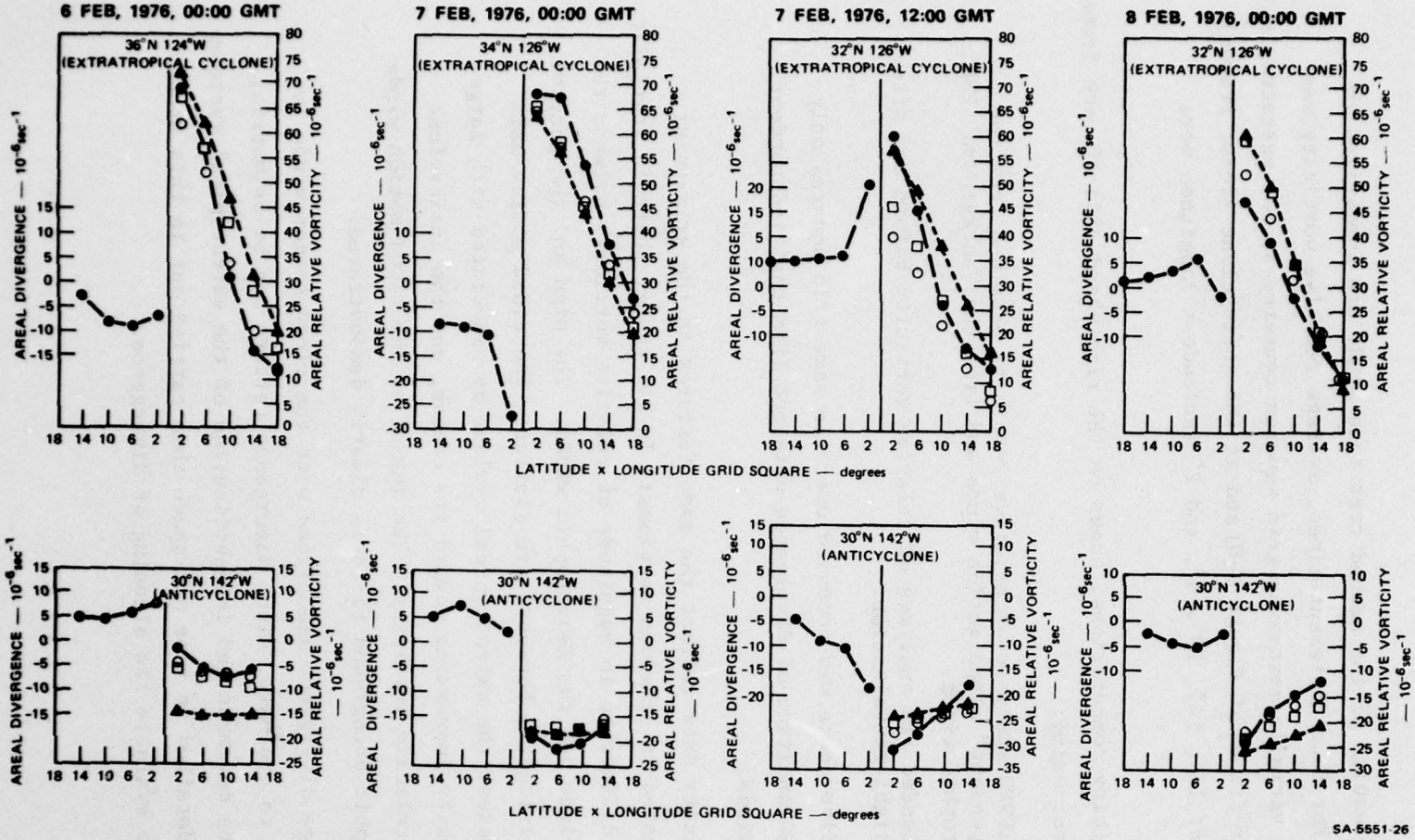

FIGURE C-8 SUMMARY OF FIB RESULTS FOR SECOND CASE STUDY, PRESENTED IN TERMS OF AVERAGE RELATIVE VORTICITY (RIGHT-HAND SIDE OF FRAMES) AND OF DIVERGENCE (LEFT-HAND SIDE OF FRAMES) COMPUTED OVER VARIABLE MESH-SIZE GRID SQUARES CENTERED AT EXTRATROPICAL CYCLONE AND ANTICYCLONE

●— —●ATSWND analysis of low-level CMV winds

▲- - -▲ATSWND analysis of FNWC 850-mb geostrophic winds

○ FIB analysis before weight reevaluation

□ FIB analysis after weight reevaluation

REFERENCES

Bauer, K. G., 1976: "A Comparison of Cloud Motion Winds with Coinciding Radiosonde Winds," Monthly Weather Rev., Vol. 104, No. 7, pp. 922-931.

Endlich, R. M., 1967: An Iterative Technique for Altering the Kinematic Properties of Wind Fields," J. Appl. Meteor., Vol. 6, No. 5, pp. 837-844.

Endlich, R. M., and R. L. Mancusco, 1968: "Objective Analysis of Environmental Conditions Associated with Severe Thunderstorms and Tornadoes," Mon. Wea. Rev., Vol. 96, No. 6, pp. 342-350.

Frankhauser, J. C., 1969: Convective Processes Resolved by a Mesoscale Rawinsonde Network," J. Appl. Meteor., Vol. 8, pp. 778-789

Gentry, C. R., T. Fujita, and R. Sheets, 1970: "Aircraft, Spacecraft, Satellite and Radar Observations of Hurricane Gladys, 1968," J. Appl. Meteor., Vol. 9, No. 6.

Gentry, R., E. Rodgers, W. E. Shenk, and V. Oliver, 1976: "Deriving Winds for Hurricanes Using Short Interval Satellite Imagery," Proceedings Seventh Conference on Aerospace and Aeronautical Meteorology and Symposium on Remote Sensing from Satellites, American Meteorological Society, November, pp. 115-118.

Hawkins, H. F., and D. T. Rubsam, 1968: "Hurricane Hilda, 1964, II. Structure and Budgets of the Hurricane on October 1, 1967," Monthly Weather Rev., Vol. 96, No. 9, pp. 617-636.

Holl, M. M., and B. R. Mendenhall, 1971: "Fields by Information Blending Sea-Level Pressure Version," Final Report, Contract N66314-70-C-5226, prepared for The Commanding Officer, Fleet Numerical Weather Central Monterey, California.

Holl, M. M., B. R. Mendenhall, and C. E. Tilden, 1971: "Technical Developments for Operational Sea Surface Temperature Analysis with Capability for Satellite Data Input," Final Report, Contract N62306-70-C-0334, prepared for Naval Weapons Engineering Support Activity Detachment (FAMOS), 3737 Branch Avenue, Room 307, Hillcrest Heights, Maryland 20031.

Mancusco, R. L., and R. M. Endlich, 1973: "Wind Editing and Analysis Program--Spherical Grid (WEAP-IA)," User's Manual, Contract DAHC04-71-C-0013, U.S. Army Research Office, Durham, N.C., Stanford Research Institute, Menlo Park, California.

Maxwell, B. R., 1976: "A Generalized Version of the Fields by Information Blending (FIB) Technique," Technical Note No. 24, Naval Environmental Prediction Research Facility, Monterey, CA 93940

O'Brien, J. J., 1970: Alternative Solutions to the Classical Vertical Velocity Problem," J. Appl. Meteor., Vol. 9, pp. 197-203.

Sasaki, Y., 1971: "A theoretical Interpretation of Anisotropically Weighted Smoothing on the Basis of Numerical Variational Analysis," Monthly Weather Rev., Vol. 99, No. 4, pp. 698-707.

Schiessl, D., 1975: "Objective Analysis Technique in Sigma Coordinates," Technical Paper No. 20-75, Naval Environmental Prediction Research Facility, Monterey, CA 93940.

Smith, C. L., 1975: "On the Intensification of Hurricane Celia (1970)," Monthly Weather Rev., Vol. 103, No. 2, pp. 131-148.

Smith, C. L., and A. F. Hasler, 1976: "A Comparison of Low-Cloud Satellite Wind Estimates and Analyses Based on Aircraft Observations in a Disturbed Tropical Regime," Monthly Weather Rev., Vol. 104, No. 6, pp. 702-708

Suchman, D., and D. W. Martin, 1976: "Wind Sets from SMS Images: an Assessment of Quality for GATE," J. Appl. Meteor., Vol. 15, No. 12, pp. 1265-1278.

Viezee, W., 1977: "Application of Satellite Microwave Radiometer Data to Weather Dynamics," Research Paper, Stanford Research Institute, Menlo Park, California, 16 March.

Yanai, M., 1961: "A Detailed Analysis of Typhoon Formation," J. Meteor. Soc. Japan, Series II, Vol. 39, No. 4, pp. 187-214.